Journal of Chemical Neuroanatomy 68 (2015) 22–38

Contents lists available at ScienceDirect

Journal of Chemical Neuroanatomy

journal homepage: www.elsevier.com/locate/jchemneu

# The centrally projecting Edinger–Westphal nucleus—I: Efferents in the rat brain

Edmilson D. Dos Santos Júnior [a,1], André V. Da Silva [a,b,f,1], Kelly R.T. Da Silva [a,b], Carlos A.S. Haemmerle [a], Daniella S. Batagello [a,d], Joelcimar M. Da Silva [a], Leandro B. Lima [e], Renata J. Da Silva [a], Giovanne B. Diniz [a], Luciane V. Sita [a], Carol F. Elias [a,c], Jackson C. Bittencourt [a,d,*]

[a] Laboratory of Chemical Neuroanatomy, Department of Anatomy, Institute of Biomedical Sciences, University of São Paulo, 05508-000 São Paulo, SP, Brazil
[b] Department of Anatomy, Institute of Biosciences, São Paulo State University, 18618-970 Botucatu, SP, Brazil
[c] Department of Molecular and Integrative Physiology, Department of Obstetrics and Gynecology, University of Michigan, Ann Arbor, MI 48109, USA
[d] Center of Neuroscience and Behavior, Institute of Psychology, University of São Paulo, 05508-030 São Paulo, SP, Brazil
[e] Department of Physiology and Biophysics, Institute of Biomedical Sciences, University of São Paulo, 05508-000 São Paulo, SP, Brazil
[f] Federal University of Mato Grosso do Sul, Três Lagoas 79600-080, MS, Brazil

ARTICLE INFO

*Article history:*
Received 31 March 2015
Received in revised form 29 June 2015
Accepted 2 July 2015
Available online 21 July 2015

*Keywords:*
Urocortin 1
Efferents
Feeding control
Corticotropin-releasing factor
Corticotropin-releasing factor receptors
Stress response

ABSTRACT

The oculomotor accessory nucleus, often referred to as the Edinger–Westphal nucleus [EW], was first identified in the 17th century. Although its most well known function is the control of pupil diameter, some controversy has arisen regarding the exact location of these preganglionic neurons. Currently, the EW is thought to consist of two different parts. The first part [termed the preganglionic EW—EWpg], which controls lens accommodation, choroidal blood flow and pupillary constriction, primarily consists of cholinergic cells that project to the ciliary ganglion. The second part [termed the centrally projecting EW—EWcp], which is involved in non-ocular functions such as feeding behavior, stress responses, addiction and pain, consists of peptidergic neurons that project to the brainstem, the spinal cord and prosencephalic regions. However, in the literature, we found few reports related to either ascending or descending projections from the EWcp that are compatible with its currently described functions. Therefore, the objective of the present study was to systematically investigate the ascending and descending projections of the EW in the rat brain. We injected the anterograde tracer biotinylated dextran amine into the EW or the retrograde tracer cholera toxin subunit B into multiple EW targets as

*Abbreviations:* 3N, oculomotor nucleus; 3V, third ventricle; 4V, fourth ventricle; 7N, facial nucleus; 7n, facial nerve; A5, noradrenergic cell group; ac, anterior commissure; Aq/aq, mesencephalic aqueduct; BDA, biotinylated dextran amine; BLA, basolateral amygdaloid nucleus anterior part; BNST, bed nucleus of the stria terminalis; BNSTov, BNST oval division; BSA, bovine serum albumin; bv, blood vessel; CART, cocaine- and amphetamine-regulated transcript; CBL, cerebellum; CC, central canal; cc, corpus callosum; CeC, central nucleus of the amygdala capsular part; CeL, central nucleus of the amygdala lateral part; CeM, central nucleus of the amygdala medial part; CG, ciliary ganglion; Cg1, cingulate cortex area 1; CGA, central gray alpha part; CLi, caudal linear nucleus of the raphe; CPu, caudate-putamen; CRF, corticotropin-releasing factor; $CRF_1$, CRF receptor subtype 1; $CRF_2$, CRF receptor subtype 2; csc, commissure of the superior colliculus; CTb, cholera toxin subunit B; cu, cuneate fasciculus; DAB, 3,3′-diaminobenzidine; Dk, Darkschewitsch nucleus; DR, dorsal raphe nucleus; DRC, dorsal raphe nucleus caudal part; DRD, dorsal raphe nucleus dorsal part; DRV, dorsal raphe nucleus ventral part; DTg, dorsal tegmental nucleus; EW, Edinger–Westphal nucleus; EWcp, Edinger–Westphal nucleus central projections; EWpg, preganglionic Edinger–Westphal nucleus; f, fornix; FG, Fluoro-Gold; gr, gracile fasciculus; HRP, horseradish peroxidase; ic, internal capsule; IL, infralimbic cortex; IO, inferior olivary nuclei; IRtA, intermediate reticular nucleus alpha part; LGP, lateral globus pallidus; LHA, lateral hypothalamic area; LHb, lateral habenular nucleus; LPB, parabrachial nucleus, lateral part; LS, lateral septal nucleus; LSi, lateral septal nucleus intermediate part; LSO, lateral superior olivary nucleus; LV, lateral ventricle; M1, primary motor cortex; MA3, medial accessory oculomotor nucleus; MCH, melanin-concentrating hormone; Me5, mesencephalic trigeminal nucleus; MeAD, medial amygdaloid nucleus anterodorsal part; mfb, medial forebrain bundle; ml, medial lemniscus; mlf, medial longitudinal fasciculus; MS, medial septal nucleus; MPB, parabrachial nucleus medial part; MPOA, medial preoptic area; mt, mammillothalamic tract; mtg, mammillotegmental tract; OB, olfactory bulb; opt, optic tract; ox, optic chiasm; PAG, periaqueductal gray matter; PAGv, periaqueductal gray matter ventral part; PaV, paraventricular hypothalamic nucleus; PBS, phosphate-buffered saline; PeF, perifornical area; pev, periventricular tract; PHA-L, *Phaseolus vulgaris* leucoagglutinin; PHD, posterior hypothalamic area; PnC, pontine nuclei; Pr5, principal sensory trigeminal nucleus; PrL, prelimbic cortex; py, pyramidal tract; Re, reuniens thalamic nucleus; RF, reticular formation; RLi, rostral linear nucleus of the raphe; RN, red nucleus; RPa, raphe pallidus nucleus; rs, rubrospinal tract; SC, superior colliculus; scp, superior cerebellar peduncle; SI, *substantia innominata*; SN, substantia nigra; SO, supraoptic nucleus; Su3c, supraoculomotor cap; UCN1-ir, urocortin 1 immunoreactivity; VA, ventral anterior thalamic nucleus; VL, ventrolateral thalamic nucles; ZI, zona incerta; ZID, zona incerta dorsal part; ZIV, zona incerta, ventral part.

* Corresponding author at: Laboratory of Chemical Neuroanatomy, Department of Anatomy ICB/USP, Av. Prof. Lineu Prestes, 2415, Lab. 106, São Paulo 05508-000, SP, Brazil. Tel.: +55 11 3091 7300; fax: +55 11 3091 8449.
*E-mail address:* jcbitten@icb.usp.br (J.C. Bittencourt).
[1] These authors contributed equally to this work.

http://dx.doi.org/10.1016/j.jchemneu.2015.07.002

controls. Additionally, we investigated the potential EW-mediated innervation of neuronal populations with known neurochemical signatures, such as melanin-concentrating hormone in the lateral hypothalamic area [LHA] and corticotropin-releasing factor in the central nucleus of the amygdala [CeM]. We observed anterogradely labeled fibers in the LHA, the reuniens thalamic nucleus, the oval part of the bed nucleus of the stria terminalis, the medial part of the central nucleus of the amygdala, and the zona incerta. We confirmed our EW–LHA and EW–CeM connections using retrograde tracers. We also observed moderate EW-mediated innervation of the paraventricular nucleus of the hypothalamus and the posterior hypothalamus. Our findings provide anatomical bases for previously unrecognized roles of the EW in the modulation of several physiologic systems.



## 1. Introduction

The Edinger–Westphal nucleus [EW] has been studied since the 17th century (Fallopius, 1600 apud Warwick, 1954), and we have learned a great deal about the cytoarchitecture, anatomy and certain connections of this nucleus since that time. Recently, further information about the neurochemical characteristics of the EW was revealed, and we have just begun to understand aspects of its function aside from its roles in the control of pupillary constriction, choroidal blood flow and lens accommodation (Gamlin and Reiner, 1991). In the late 1990s, two new neuropeptides were discovered, urocortin 1 [UCN1—Vaughan et al., 1995; in the present study, we will follow the nomenclature for receptors of corticotropin-releasing factor – CRF – and their ligands that was proposed by Hauger et al., 2003], and cocaine- and amphetamine-regulated transcript [CART—Douglass and Daoud, 1996; Koylu et al., 1998]. UCN1 was subsequently mapped in the rat brain (Bittencourt et al., 1999; Kozicz et al., 1998). The primary sites of UCN1 mRNA expression and protein immunoreactivity are the EW and the lateral superior olivary nucleus [LSO], and UCN1-immunoreactive [UCN1-ir] fibers are broadly distributed throughout the CNS from the prosencephalon to the spinal cord of the albino rat. CART is also found in EW neurons. However, both UCN1 and CART are expressed in other brain areas, and the EW contains neurons that express other neuromodulators. Maciewicz et al. (1983, 1984) described in the cat that, the EW neurons projecting to the spinal cord and the cerebellum contain substance-P, and those projecting to the caudal trigeminal nucleus and spinal cord, as well, contain cholecystokinin.

Most of our previous understanding of the EW in terms of the colocalization of neurotransmitters and neuropeptides in its neurons and the connections and related functions of this nucleus has been revised. Indeed, the view that the EW represents a specific cluster of cholinergic cells began to change with the work of Strassman et al. (1987); in this study injections of horseradish peroxidase [HRP] into the ciliary ganglion [CG] of the cat combined with measurements of choline acetyltransferase immunoreactivity revealed that the majority of the double-labeled cells were outside the classical boundaries of the EW and that several of these cells were not even cholinergic. Although many studies have described the phylogeny, anatomy, cytoarchitecture, neurochemical aspects and functional roles of the EW, few studies have explored its connectivity. Most of the studies that have been performed to establish its connections have used retrograde tracers and/or lesions of the CG (Akert et al., 1980; Burde and Loewy, 1980; Crouch, 1936; Ishikawa et al., 1990; Warwick, 1954) [see Kozicz et al., 2011, for a comprehensive review]. Loewy and Saper (1978) used [$^3$H]-labeled amino acids as an anterograde tracer in cats to define the following brainstem targets of the EW: the dorsal accessory nucleus, the parabrachial nucleus, the subtrigeminal nucleus, the spinal trigeminal nucleus, the gracile and medial cuneate nuclei, and certain layers of the spinal cord. Klooster et al. (1993) used *Phaseolus vulgaris* leucoagglutinin [PHA-L] to identify terminal projections from the EW to the ipsi- and contralateral olivary complex nuclei, the lateral parabrachial nucleus, the facial nucleus, the trigeminal brainstem nuclear complex, the lateral reticular nucleus, the rostroventral reticular nucleus, and the CG. However, the authors of this study did not describe any ascending projections from the EW. Bittencourt et al. (1999) demonstrated for the first time that the EW does indeed send ascending projections, specifically to the lateral septal nucleus, and confirmed the previously known projections from the EW to the spinal cord.

Studies have suggested the existence of at least two subdivisions of the EW based on neurochemistry or function: (1) the preganglionic EW [EWpg], which is composed of a group of cholinergic neurons that induce pupillary constriction and lens accommodation; (2) the centrally projecting EW [EWcp], which contains a group of peptidergic neurons that have been related to feeding behavior, stress response, addiction and pain control (Kozicz et al., 2011; May et al., 2008; Vasconcelos et al., 2003). Moreover, our group has described the connection between the lateral hypothalamic area [LHA] and the EW, as well as between the medial part of the central nucleus of the amygdala [CeM] and the EW (da Silva et al., 2013) by injecting a retrograde tracer into the EW. Since this finding, we have searched for the connections between the EW and areas related to feeding behavior and stress response. It would be of interest to determine whether these efferents from the EW connect to neurons with known biochemical signatures, such as the melanin-concentrating hormone [MCH] and corticotropin-releasing factor [CRF], in these two areas [LHA and CeM]. There is also evidence that the EW includes dopamine-containing neurons and that the EW may be related to the alcohol addiction behavior, as indicated in the study by Bachtell et al. (2002).

However, due to the lack of studies directly examining the projections of the EW, it has been difficult to elucidate the roles of EW neurons in physiology and behavior. Therefore, in the present study, we aimed to systematically describe the efferents of the EW using standard neuronal tracers combined with neurochemical tools to shed light on its potential downstream targets and related functions.

## 2. Materials and methods

### 2.1. Animals

Adult male Long–Evans rats weighing 300–330 g were housed two per cage in the animal care facility of our institution and were allowed to adapt for at least seven days prior to the initiation of the experiments. The animals were maintained on a 12-h/12-h light/dark cycle [lights on at 7:00 am] in a temperature-controlled environment [21 ± 2 °C] and were provided with access to water and rat chow *ad libitum*. All experiments were performed in accordance

with the Guidelines for the Care and Use of Mammals in Neuroscience and Behavioral Research established by the National Research Council (2003) and with the guidelines established by the University of São Paulo Institute of Biomedical Sciences Committee for Ethics and Animal Care in Experimental Research, which approved this study [Protocol no. 040/2003]. All efforts were made to minimize the number and suffering of animals used in the experiments. The rats were divided into three groups according to the methodology employed: cytoarchitecture and neurochemistry [$N = 10$], anterograde tracer injection [$N = 68$], and retrograde tracer injection [$N = 34$].

### 2.2. Antisera characterization

The antisera used in this study, which have been previously characterized in other studies, specifically label the expected group of cells. Please see Table 1 for additional information regarding the antisera used in the present study. The staining specificity was confirmed by omitting the primary antibodies and using negative and positive controls in normal goat serum and normal donkey serum. The antisera controls were negative in all tests.

### 2.3. Anterograde tracer injection

Biotinylated dextran amine [BDA, 10%] diluted in distilled water was used to identify the EW projections. Sixty-eight rats received an iontophoretic injection of BDA into the EW. The BDA was deposited via a glass micropipette with a 10–20 μm tip diameter by applying a +5 μA current, pulsed at 7-s intervals, with a constant-current source [Midgard Electronics, Watertown, MA, USA], during a 15 min period, The coordinates of the EW were as follows: AP, −5.2; ML, 0.0; and DV, 5.9 [considering Bregma as a point of reference for these coordinates]. Two weeks later, the rats were anesthetized, transcardially perfused and sliced as described below. The sections were examined for tracer deposition, and the fibers were visualized using an avidin–biotin peroxidase kit [Vectastain Elite, Vector Labs, Burlingame, CA, USA] followed by a peroxidase reaction using diaminobenzidine [DAB] as the chromogen.

### 2.4. Localizing the site of BDA injection into the EW UCN1-ir cells

Immunofluorescence double-labeling was used to verify whether the BDA injections targeted the EW UCN1-ir cells. The sections were washed twice in 0.02 M KPBS for 10 min each and treated with 0.3% hydrogen peroxide for 15 min. After rinsing with KPBS, the sections were pretreated with a solution containing 0.3% of hydrogen peroxide in KPBS containing 0.3% Triton X-100 for 30 min. Then, the sections were rinsed in KPBS and processed for immunofluorescence using an anti-rUCN1 antibody [see Table 1 for antisera details] in KPBS containing 1% BSA, 0.0056% heparin and 0.25% Triton X-100 for approximately 18 h. Approximately 24 h later, the sections were rinsed in KPBS and incubated for 1 h in Cy3-conjugated donkey anti-goat IgG antiserum [Jackson Laboratories, West Grove, PA, USA] at 1:200. Next, the sections were rinsed again in KPBS and processed according to a streptavidin fluorescence protocol. Then, the sections were incubated in a solution containing KPBS, 0.3% Triton X-100, 2% normal goat serum and fluorescein [DTAF]-conjugated streptavidin [1:200; Jackson Laboratories] for 2 h. Then, the sections were rinsed in KPBS, mounted on gelatin-coated slides and coverslipped with buffered glycerol mountant [pH 8.5].

### 2.5. Retrograde tracer control injections

Cholera toxin subunit B [CTb—List Biological Laboratories, Campbell, CA, USA] diluted in distilled water [1%] was used for the

**Table 1**
Primary antibodies used in the experiments.

| Common name of antibody | Manufacturer | Number or code | Reference (first author, volume: pages, year and journal) | PubMed ID | Antibody ID from NIF | Antibody link | Amino acids position | Dilution |
|---|---|---|---|---|---|---|---|---|
| Rabbit anti rat melanin-concentrating hormone (anti-rMCH) DFDMLRCMLGRVYRPCWQV | Peptide Biology Laboratory, Dr. Joan Vaughan | PBL #234 | Nahon, JL., 125(4): 2056–2065, 1989 (Endocrinology) | 2477226 | – | – | | 1:25,000 (peroxidase) 1:1000 (fluorescence) |
| Rabbit anti rat urocortin 1 (anti-rUCN1) | Peptide Biology Laboratory Dr. Joan Vaughan | PBL #5779 | Vaughan, J., 378(6554): 287–292, 1995 (Nature) | 7477349 | – | – | – | 1:1,000 (fluorescence) 1:2000 (peroxidase) |
| Rabbit anti rat corticotropin-releasing factor (anti-rCRF) | Peptide Biology Laboratory Dr. Joan Vaughan | PBL #C70 | Sawchenko, P.E., 4(4): 1118–1129, 1984 (J. Neurosci) | 6609226 | – | – | – | 1:3000 (peroxidase) |
| Rabbit anti-fluorogold (anti-FG) | Millipore-Chemicon | AB-153 | Zappone, C.A., 24(4): 853–864, 2004 (J. Neurosci.) | 14749430 | AB_90738 | http://antibodyregistry.org/AB_90738 | – | 1:60,000 (peroxidase) |
| Goat anti cholera toxin B-subunit (anti-CTb) | List Biological Laboratories, Inc. | #703 | Cavalcante, J.C., 1089(1): 116–125, 2006 (Brain Res.) | 16638605 | AB_10013220 | http://antibodyregistry.org/AB_10013220 | – | 1:60,000 (peroxidase) 1:3000 (fluorescence) |

retrograde tracer injection control experiments. Nine rats received an iontophoretic injection of CTb into the LHA [$n = 3$] or the CeM [$n = 6$]. CTb was injected via a glass micropipette with a 20-μm tip diameter, by applying a +5 μA current, pulsed at 7-s intervals, with a constant-current source [Midgard Electronics, Watertown, MA, USA], during a 5 min period. The stereotaxic coordinates were as follows: LHA, AP: −2.0; ML: 1.5; DV: 7.6; CeM, AP: −2.0; ML: 13.8; DV: 6.5. After 2 weeks, the rats were anesthetized and transcardially perfused, and sections were sliced according to the following description. The sections were pretreated with 0.3% hydrogen peroxide solution in KPBS containing 0.25% Triton X-100 for 1 h, followed by incubation in normal goat serum [2%] for 1 h. Next, the tissues were incubated in a goat anti-CTb primary antibody [1:60,000] [List Biological] overnight. The next day, after rinsing with KPBS [2 × 10 min], the sections were incubated in a biotin-conjugated donkey anti-goat IgG secondary antibody [1:1000, Jackson Laboratories] for 1 h. After washing with KPBS [2 × 10 min], the sections were incubated in the avidin–biotin complex [1:250; Vector Labs] for 1 h followed by peroxidase and 0.05% DAB as the chromogen. An additional group of rats [$n = 25$] received a stereotaxic injection of the retrograde tracer Fluoro-Gold [FG; 2% in saline; Fluorochrome, Englewood, CO, USA] into the LHA. Our aim was to identify the EW neurons that were retrogradely labeled and UCN1-positive and to compare the efficacies of the CTb and FG tracers when injected at the aforementioned coordinates. Each tracer was iontophoretically injected using a glass micropipette [internal diameter, 10 μm] via the application of a +5 μA current pulsed at 7-s intervals for 10 min. After 15 days, the animals were perfused, and the brains were sectioned as described below. To identify the injection site, the sections were mounted on gelatin-coated slides, coverslipped with buffered glycerol mounting medium [pH 8.5] and evaluated via epifluorescence microscopy using a UV filter [340–380 nm]. An adjacent series of sections was stained with thionin to serve as a cytoarchitecture reference. Another series of sections from the animals whose injections were restricted to the LHA was used for immunofluorescence staining using a rabbit primary anti-UCN1 antibody for 48 h at 4 °C. After rinsing with KPBS, the sections were incubated for 1 h in a fluorescein isothiocyanate-conjugated goat anti-rabbit secondary antiserum [Jackson Laboratories] diluted to 1:200. Next, the sections were washed in KPBS [2 × 10 min], mounted on gelatin-coated slides and coverslipped with buffered glycerol medium.

### 2.6. Identifying EW target regions with known biochemical signatures

A double avidin–biotin immunoperoxidase kit [Vectastain Elite, Vector Labs] was used to detect MCH-ir cells in the LHA and CRF-ir cells in the CeM putatively receiving innervation from the BDA-stained fibers from the EW nucleus. The sections were pretreated with 0.3% hydrogen peroxide solution and incubated in the avidin–biotin complex [1:250] diluted in KPBS for 1 h. Then, the sections were rinsed with KPBS and subjected to a peroxidase reaction using DAB and nickel sulfate [Thermo Fisher Scientific Inc., Waltham, MA, USA] as the chromogen solution. Next, the tissue was incubated in KPBS containing Triton X-100 and normal goat serum [2%] for 1 h followed by the primary anti-MCH or anti-CRF antibody diluted in the same solution for ∼18 h [see Table 1 for details of the antisera used in this work] (Bittencourt et al., 1992; Nahon et al., 1989; Sawchenko et al., 1984). After rinsing in KPBS, the sections were incubated in a biotin-conjugated goat anti-rabbit IgG secondary antibody [1:1000] for 1 h. Next, the sections were rinsed in KPBS [2 × 10 min] and then incubated in avidin–biotin complex [1:250] for 1 h. Finally, the sections were subjected to a peroxidase reaction using DAB as the chromogen in the absence of nickel sulfate.

### 2.7. Animal perfusion and histology

After anesthetization using 1 ml of chloral hydrate [35%, i.p.], the animals were transcardially perfused with ∼100 ml of cold saline 0.9% [for ∼1 min] followed by 700–900 ml of 4% formaldehyde [obtained from paraformaldehyde heated at 60–65 °C] in borate buffer, pH 9.5, at 4 °C for ∼25 min. Immediately after perfusion, the brain and the spinal cord were removed from the skull and post-fixed using the same fixative solution containing 20% sucrose at 4 °C for 4 h; subsequently, these samples were transferred to 20% sucrose in phosphate-buffered saline [PBS] for approximately 18 h at 4 °C for cytoarchictectonic and neurochemical assessment or to 20% sucrose in the same fixative for approximately 18 h at 4 °C for tracer examination. The brain and the spinal cord were sectioned in the coronal and transversal planes [30 μm], respectively, using a freezing microtome, and the sections were stored in anti-freezing solution at −30 °C. To study the EW structure, the surrounding nuclei and tracts in one series of sections from each animal were Nissl-stained [thionin 0.025%].

### 2.8. Imaging

Photomicrographs were captured with a digital camera [Nikon Corporation, Chiyoda, Tokyo, Japan] coupled to a Leica DMR microscope [Leica Microsystems, Wetzlar, Germany] using NIS-Elements BR 3.0 [Nikon]. The schematic drawings of the BDA and CTb injection sites were created using Canvas X® software. All images were adjusted for sharpness, contrast and brightness using Adobe Photoshop CS2. Fig. 4 was created using Adobe Illustrator CS5.

### 2.9. Analysis of the results

We mapped the BDA-labeled fibers observed via light microscopy using semi-quantitative comparative analyses. The number of plus signs represents the density of BDA-labeled fibers [see Fig. 1 for examples]. We defined satisfactory injections as those which were located within the EW according to an atlas (Paxinos and Watson, 2007) and as evidenced by the labeling of UCN1-ir cells, which characterize a subdivision of the EW (Bittencourt et al., 1999; Kozicz et al., 1998).

## 3. Results

### 3.1. Nomenclature

The EW is immediately ventral to the mesencephalic aqueduct [Aq], occupies the median line of the periaqueductal gray matter [PAG], and approximately corresponds to the coordinates noted in the rat brain atlas [between −5.20 mm and −6.84 mm to Bregma] (Paxinos and Watson, 2007). Importantly, UCN1-/CART-ir cells are detectable rostral to this boundary [−5.20], between the two fasciculi retroflexus, and ventral to the dorsal part of the third ventricle [3V], which transitions into the Aq in the posterior hypothalamic area [PHD] (Bittencourt et al., 1999). As mentioned above, in the present report, we employ the term EW for both parts of the recently described nucleus [i.e., the EWcp and the EWpg] (Kozicz et al., 2011) because it is unavoidable to inject both parts of the EW with standard tracers given its cytoarchitecture. Interestingly, only the injections into the ventral portion of the parallel columns of the EW that were localized medial to the oculomotor nucleus [3N] and that contaminated the most medial aspects of the 3N revealed fibers exiting the oculomotor complex and adjoining the oculomotor nerve [data not shown].

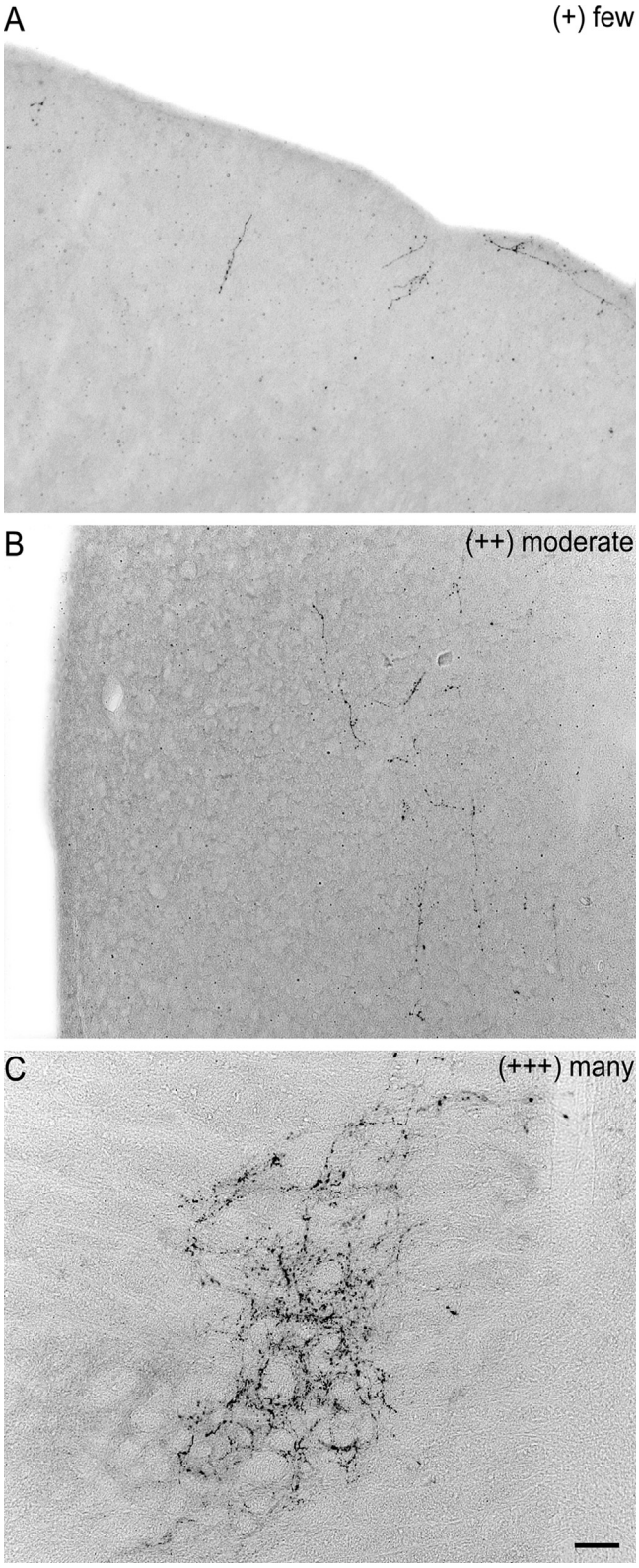


**Fig. 1.** Distribution of BDA-labeled fibers. The number of plus signs represents the density of BDA-labeled fibers in three regions of the rat CNS. Brightfield photomicrographs of immunoperoxidase staining demonstrating anterogradely labeled fibers distributed in different regions are presented to guide the reader concerning the several other nuclei mentioned in the text and in Table 2 as follows: (A) "few" [+]; (B) "moderate" [++]; and (C) "many" [+++]. Scale bar = 50 μm.

### 3.2. Anterograde tracer injection

Sixty-eight stereotaxic injections of BDA were performed. Six cases were found to be satisfactory and were used for mapping [cases LE#61, LE#66, LE#69, LE#89, LE#103 and LE#104—Fig. 2]. Four of these cases, i.e., LE#61, LE#66, LE#69 and LE#89, were at the intermediate level, but minimally contaminated the medial borders of the 3N. The precise localization of BDA injections is shown for LE#61 and LE#69 [Fig. 3A and B, respectively]. Two cases [LE#103 and LE#104] were within the boundaries of the EW but included larger areas than the former four cases. Both of these injections displayed greater dorsal–ventral extents and therefore encompassed neighboring structures, such as the ventral part of the PAG [PAGv], the supraoculomotor part of the PAG and the 3N itself. Moreover, in these two cases the projections from the EW to all CNS regions were denser than those in the other four cases. Any case, in which the injection stained at least one of the parallel columns of the EW, independent of the rostrocaudal level, were considered as good injections. Additionally, due to concerns about the boundaries and the cytoarchitecture of the EW with respect to the injection sites, we decided to verify the exact locations of the BDA injections [Fig. 3A″ and B″] based on neurochemical organization, i.e., the distribution of UCN1-ir cells [Fig. 3A′ and B′], via immunohistochemical double-labeling [Fig. 3A‴ and B‴] of cases LE#61 and LE#69. In this study, we used case LE#61 as an example to describe the projections from the EW because the other three cases exhibited similar amounts of BDA transport and density of the BDA-labeled projections in the terminal fields. The complete distributions of the anterogradely labeled fibers are presented in Table 2. Subsequently, we describe the four divisions of the CNS of the Long-Evans rat in terms of the nuclei in which we observed labeled fibers. Since we do not yet have a well established method to quantify labeled fibers, we performed qualitative assessments of the anterogradely labeled fibers representing the amount of innervation of a certain CNS region, area or nucleus. Based on this premise, we selected specific brain regions representing low, moderate and high levels [Fig. 1A–C, respectively] of anterogradely labeled fibers to serve as a guide to the reader to facilitate the appropriate interpretation of Table 2.

#### 3.2.1. The pathways to the targets

Following BDA injection into the EW, fibers exhibiting varicosities and characteristic terminal boutons with distinct directions were noted. Some of the fibers followed fascicles, such as the medial longitudinal fasciculus [mlf], or followed the dorsal border of the PAG near the Aq, primarily in the PAGv. Other fibers were observed to cross the PAG and project to the tectum or remain diffusely distributed in the local white matter [Fig. 4—red tracing]. To reach diencephalic territories some of the efferents from EW use the periventricular tract [Fig. 4—yellow tracing]. Some long axonal projections were organized ventrolaterally toward the mesencephalic reticular formation [RF] [Fig. 4—green tracing], whereas others crossed or bordered the red nucleus [RN] and proceeded to the medial lemniscus [ml] [Fig. 4—orange tracing] or the medial forebrain bundle [mfb] [Fig. 4—blue tracing]. The medially localized axonal projections crossed the dorsal raphe nucleus, and some of these projections extended deeper into the white matter or reached nuclei in the surrounding brainstem region. Therefore, following BDA injection, we observed that the fibers were organized into two principal routes; the first route extended upwardly toward the prosencephalon, and the second route extended downward to the brainstem and the spinal cord.

*3.2.1.1. The three ascending fiber pathways. Periventricular tract [pev—yellow tracing]:* These fibers projected parallel to the Aq until it became the 3V and then spread up to the medial nuclei of the

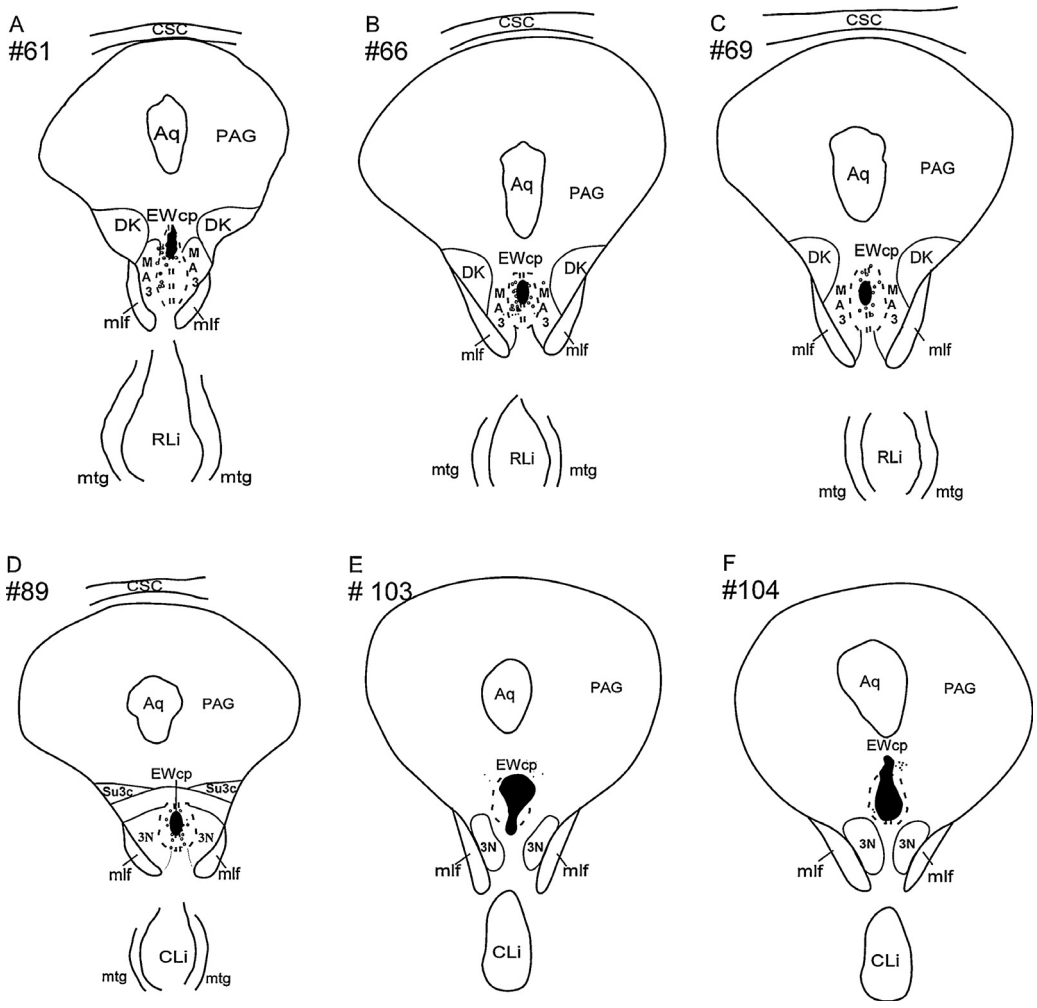


**Fig. 2.** Diagram showing representative BDA injection sites in the EW. Schematic drawings showing the six cases that were considered to be good injections [the dotted, dark areas represent the BDA injection sites]: (A) case LE#61; (B) case LE#66; (C) case LE#69; (D) case LE#89; (E) case LE#103; and (F) case LE#104. For abbreviations, see the list.

hypothalamus in the periventricular region and to the medial nuclei of the thalamus located at the rostral edge of the 3V [Fig. 4].

*Medial lemniscus [ml—orange tracing]:* The BDA fibers extended along the ascending pathway of this bundle until near the thalamic nuclei. In this route, we noted that the zona incerta [ZI], LHA and ventral thalamic nuclei received many BDA fibers that followed the *ml* and remained in this region until the rostral edge of the diencephalon [Fig. 4].

*Medial forebrain bundle [mfb—blue tracing]:* We observed that the fibers from the EW that extended in the ventrolateral direction followed the *mfb*. These fibers were well visualized in the base of the posterior [mammillary] part of the LHA and crossed the rostrocaudal axis of the diencephalon. At the rostrocaudal level of the anterior hypothalamic nuclei, these fibers bordered the base of the median preoptic nucleus and extended along the midline toward the septal nuclei. In this location, the fibers maintained their previous route toward the infralimbic cortex [IL] and the cingulate cortex [Cg1], where we observed the greatest numbers of ascending fibers [Fig. 4].

*3.2.1.2. The descending fiber pathways. Midbrain, pons, medulla oblongata and spinal cord*

*Medial longitudinal fasciculus [mlf—red tracing]:* Some crossing fibers were observed in the *mlf* that extended until the formation of the oculomotor nerve, and no fibers were observed below this level [Fig. 4]. In the ventral region of the Aq [red tracing], some fibers remained ventral to the Aq until the fourth ventricle [4V], and some of these fibers crossed to innervate the layers of the superior colliculus. At this level, some fibers accompanied the opening of the 4V, spread into local nuclei to laterally extend toward the parabrachial nuclei, and further descended to the rostral part of the solitary complex [Fig. 4]. In the pathways to the reticular formation [green tracing], some fibers, including long transverse and ventrolateral projections, spread into the mesencephalic RF, from which they were distributed along the midline. These fibers exhibited the same characteristics while extending along the rostrocaudal axis of the pontine RF. However, as these fibers extended further into the white matter of the pons, they were clustered on the edges of the RF until the level of the A1 catecholaminergic cell group in the medulla oblongata [Fig. 4].

*Spinal cord [green tracing]:* At the level of the spinal cord, we detected fibers descending into the dorsolateral fasciculus to enter the gray matter in the very first layers going toward the intermediolateral and intermediomedial cell columns and ventral horn. Varicose fibers, fibers of passage and terminal boutons were observed in all layers but were primarily located in laminae I, II, III, VII, VIII and X [Fig. 4].

### 3.3. Prosencephalon

A few BDA fibers were found in the orbital cortex, the anterior olfactory nucleus, the pre- and infralimbic cortices, the cingulate

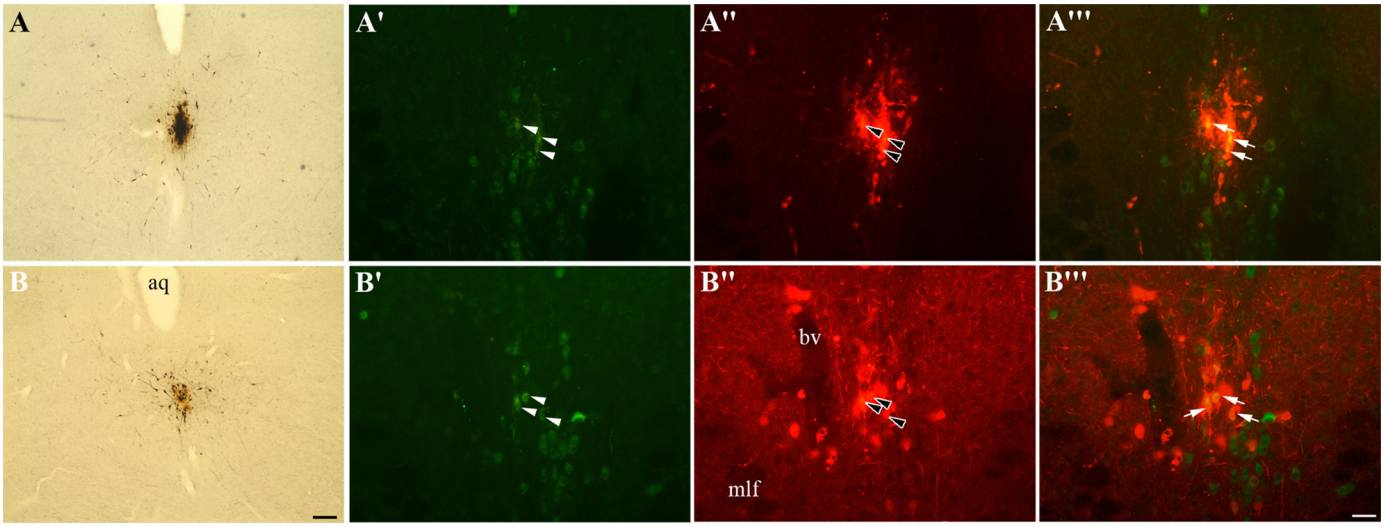


**Fig. 3.** Examples of BDA injection sites in the EW. Histochemical peroxidase staining and fluorescent photomicrographs of the BDA injection sites into the EW in two representative cases [(A) LE#61 and (B) LE#69]. (A and B) small circumscribed BDA injections were revealed by histochemical peroxidase staining in the EW, demonstrating that BDA labeling was limited to the boundaries of the EW; (A′ and B′) sections from an adjacent series showing UCN1-ir [Cy2—green] in the EW [white arrowheads] under a blue light filter; (A″ and B″) the same sections under a green light filter [Cy3—red] showing the BDA injection sites [black arrowheads with white contour]. (A‴ and B‴) overlay of the two images described immediately beforehand showing that the BDA injection sites indeed targeted UCN1-ir cells in the EW [the cells that absorbed the tracer are labeled in yellow-gold–white arrows]. For abbreviations, see the list. Scale bars: A and B = 100 μm; A′, A″, A‴, B′, B″, and B‴ = 50 μm (For interpretation of the references to color in this figure legend, the reader is referred to the web version of this article.).

gyrus [Fig. 5A], the anterior amygdaloid area, and the basolateral amygdaloid nucleus [BLA] [Fig. 5D]. The following areas exhibited moderate numbers of BDA-labeled fibers: the medial septal nucleus [MS] and the lateral septal nucleus, intermediate part [LSi] [Fig. 5C]; the horizontal and vertical limbs of the diagonal band of Broca; the anterodorsal part of the bed nucleus of the stria terminalis [BNST]; the *substantia innominata*; and the ventral pallidum. Moderate to large numbers of anterogradely labeled fibers were observed in the CeM and in the oval part of the BNST [BNSTov] [Fig. 5D and B, respectively].

### 3.4. Diencephalon

In the diencephalon, we observed anterogradely labeled fibers in the following regions with the respective densities: very few fibers: the anterior parvocellular part of the paraventricular nucleus of the hypothalamus [PaV]; few fibers: the medial preoptic area, the preoptic magnocellular nucleus, the subparaventricular zone of the hypothalamus, the dorsomedial nucleus of the hypothalamus, the supraoptic nucleus [SO] [Fig. 6G and H], the centrolateral nucleus of the thalamus, the ventro-anterior and ventro-lateral nuclei of the thalamus, the parafascicular nucleus of the thalamus, the lateral habenular nucleus; few to moderate numbers of fibers: the lateral preoptic area, the perifornical area [PeF], the periventricular hypothalamic nucleus, the PHD [dorsal part] [Fig. 6C and D], the mediodorsal thalamic nucleus, the centromedial thalamic nucleus, the interoanteromedial thalamic nucleus, the rhomboid nucleus of the thalamus, the posterior part of the paraventricular nucleus of the thalamus, the ventromedial thalamic nucleus, the laterodorsal thalamic nucleus, the intermediodorsal thalamic nucleus, and the posterior nucleus of the thalamus; and moderate to high numbers of fibers: the LHA [Fig. 6E and F], the ZI [Fig. 6A and B], and the reuniens thalamic nucleus [Re] [Fig. 6C and D].

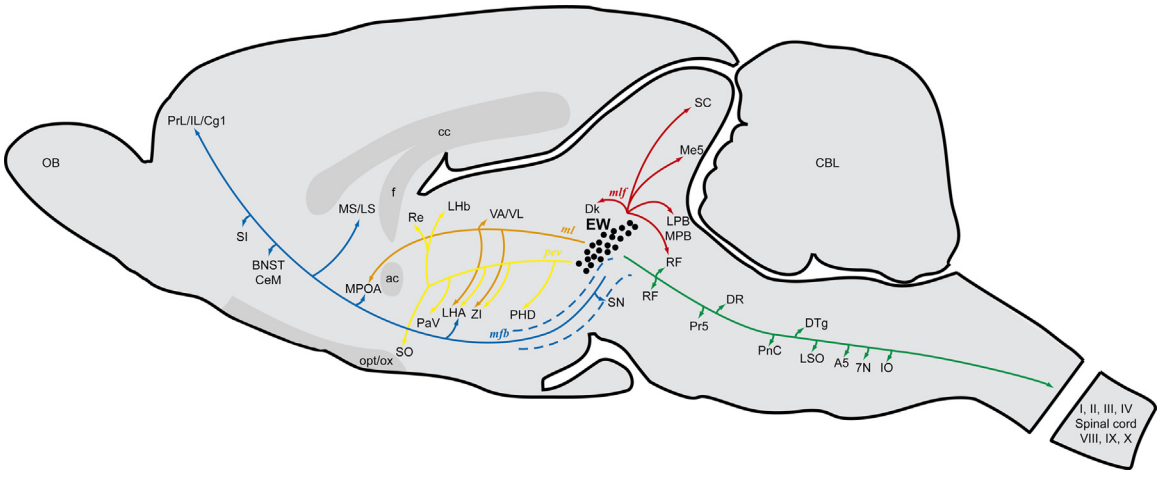


**Fig. 4.** Schematic drawing of a sagittal section of the rat brain demonstrating the EW centrally projections after BDA injection into it. The EW is represented by several black dots while the ascending and descending pathways originated from it are indicated in different colors. Ascending pathways: orange, medial lemniscus; yellow, periventricular tract; blue, medial forebrain bundle. Descending pathways: red, medial longitudinal fasciculus; green, to brainstem nuclei and spinal cord. For abbreviations, see the list (For interpretation of the references to color in this figure legend, the reader is referred to the web version of this article.).

**Table 2**
Relative density evaluation of anterogradely labeled fibers following successful BDA injections into the EW.

| CNS regions | Relative density | CNS regions | Relative density |
|---|---|---|---|
| I. Prosencephalon | | | |
| Anterior amygdaloid area | + | Nucleus of the horizontal limb of the diagonal band | +/++ |
| Anterior olfactory nucleus | −/+ | Nucleus of the vertical limb of the diagonal band | +/++ |
| Basolateral amygdaloid nucleus | + | Orbital cortex | −/+ |
| Bed nucleus of the stria terminalis, lateral division | ++ | Piriform cortex | + |
| Central nucleus of amygdala | ++ | Prelimbic/infralimbic cortex | + |
| Cingulate cortex | + | *Substantia innominata* | +/++ |
| Lateral septal nucleus, intermediate part | +/++ | Ventral pallidum/olfactory tubercle | +/++ |
| Medial septal nucleus | **+/++** | | |
| II. Diencephalon | | | |
| Anterior hypothalamic area | ++ | Paracentral thalamic nucleus | ++/++ |
| Central medial thalamic nucleus | ++ | Parafascicular thalamic nucleus | + |
| Centrolateral thalamic nucleus | + | Paraventricular hypothalamic nucleus, anterior parvicellular part | −/+ |
| Dorsal tuberomammillary nucleus | ++ | Paraventricular thalamic nucleus, posterior part | +/++ |
| Dorsomedial hypothalamic nucleus | + | Perifornical area | +/++ |
| External medullary lamina | + | Periventricular hypothalamic nucleus | +/++ |
| Lateral habenular nucleus | + | Posterior hypothalamic area | +/++ |
| Interanteromedial thalamic nucleus | ++ | Posterior complex of the thalamus | +/++ |
| Intermediodorsal thalamic nucleus | +/++ | Reuniens thalamic nucleus | ++/+++ |
| Lateral hypothalamic area | ++/+++ | Rhomboid thalamic nucleus | ++ |
| Lateral preoptic area | +/++ | Subparaventricular zone of the hypothalamus | + |
| Laterodorsal thalamic nucleus | ++ | Ventral anterior thalamic nucleus | + |
| Magnocellular preoptic nucleus | + | Ventrolateral thalamic nucleus | + |
| Medial preoptic area | + | Ventromedial thalamic nucleus | +/++ |
| III. Brainstem | | | |
| A5 noradrenaline cells | + | Oculomotor nucleus, parvicellular part | +/++ |
| A8 dopamine cells | +/++ | Paragigantocellular nuclei | + |
| Accessory facial nucleus | + | Paramedian raphe nucleus | + |
| Anterior tegmental nucleus | −/+ | Pararubral nucleus | +/++ |
| Barrington's nucleus | + | Parvicellular reticular nucleus | +/++ |
| Caudal linear nucleus of the raphe | +/++ | Parvicellular reticular nucleus, alpha part | + |
| Central gray, alpha part | + | Pontine nuclei | + |
| Deep layers of the superior colliculus | ++ | Pontine reticular nucleus | ++ |
| Deep mesencephalic nucleus | ++ | Precommissural nucleus | + |
| Dorsal raphe nucleus | +/++ | Prerubral field | +/++ |
| Dorsolateral periaqueductal gray | + | Pretectal nuclei | +/++ |
| Dorsolateral periaqueductal gray | + | Principal sensory trigeminal nucleus | −/+ |
| Facial nucleus | + | Raphe interpositus nucleus | + |
| Gigantocellular reticular nucleus | +/++ | Raphe magnus nucleus | −/+ |
| Inferior olivary nuclei | +++ | Raphe obscurus nucleus | + |
| Intermediate reticular nucleus | + | Raphe pallidus nucleus | + |
| Interstitial nucleus of medial longitudinal fasciculus | ++ | Retrorubral field | + |
| Lateral parabrachial nucleus | + | Rostral linear nucleus of the raphe | + |
| Lateral periaqueductal gray | + | Subcoeruleus nucleus | −/+ |
| Medial accessory oculomotor nucleus | +/++ | Substantia nigra, compact part | ++ |
| Medial parabrachial nucleus | + | Substantia nigra, reticular part | + |
| Mesencephalic trigeminal nucleus | +/++ | Superficial layer of the superior colliculus | + |
| Nucleus of Darkschewitsch | ++ | | |
| Nucleus of the fields of Forel | + | Supraoculomotor (periaqueductal gray and cap) | +/++ |
| Nucleus of the posterior commissure | +/++ | Ventral tegmental area | + |
| Nucleus of the solitary tract | ++ | Ventrolateral periaqueductal gray | ++ |
| Oculomotor nucleus | −/+ | | |
| **IV.** Spinal cord | | | |
| Lamina I | + | Lamina VI | − |
| Lamina II | + | Lamina VII | + |
| Lamina III | + | Lamina VIII | + |
| Lamina IV | + | Lamina IX | + |
| Lamina V | − | Lamina X | + |

### 3.5. Brainstem

Small numbers of anterogradely labeled fibers were detected in the A5 group of noradrenergic cells [Fig. 7B] and in the following nuclei: the 3N, the anterior tegmental nucleus, the raphe magnus nucleus, the *subcoeruleus* nucleus, and the principal trigeminal nucleus. However, the primary brainstem nuclei that exhibited moderate numbers of anterogradely labeled fibers were the following: the substantia nigra *pars compacta*, the deep mesencephalic nucleus, the interstitial nucleus of the medial longitudinal fasciculus, the periaqueductal gray matter pars anterior and ventrolateral, the Darkschewitsch nucleus, the deep layers of the superior colliculus, the reticular pontine nucleus, and the dorsal raphe nucleus [ventral and dorsal parts, DRV and DRD, respectively] [Fig. 7A]. The most densely innervated nucleus of the brainstem appeared to be the inferior olivary nuclei [IO] [Fig. 7E], therefore, we have given to it three pluses, following Fig. 1. The ventral tegmental area exhibited few to moderate numbers of anterogradely labeled fibers. We also observed BDA fibers in the facial nucleus [7N] [Fig. 7D], the mesencephalic trigeminal nucleus, and the dorsal tegmental nucleus [DTg] [Fig. 7C]. The parabrachial nucleus [medial and lateral parts] was observed to contain just a few BDA-labeled fibers [Fig. 7F]. We did not observe anterogradely labeled fibers in any part of the cerebellum. See Table 2 for a complete list of the rat CNS regions and nuclei in which BDA fibers were observed.

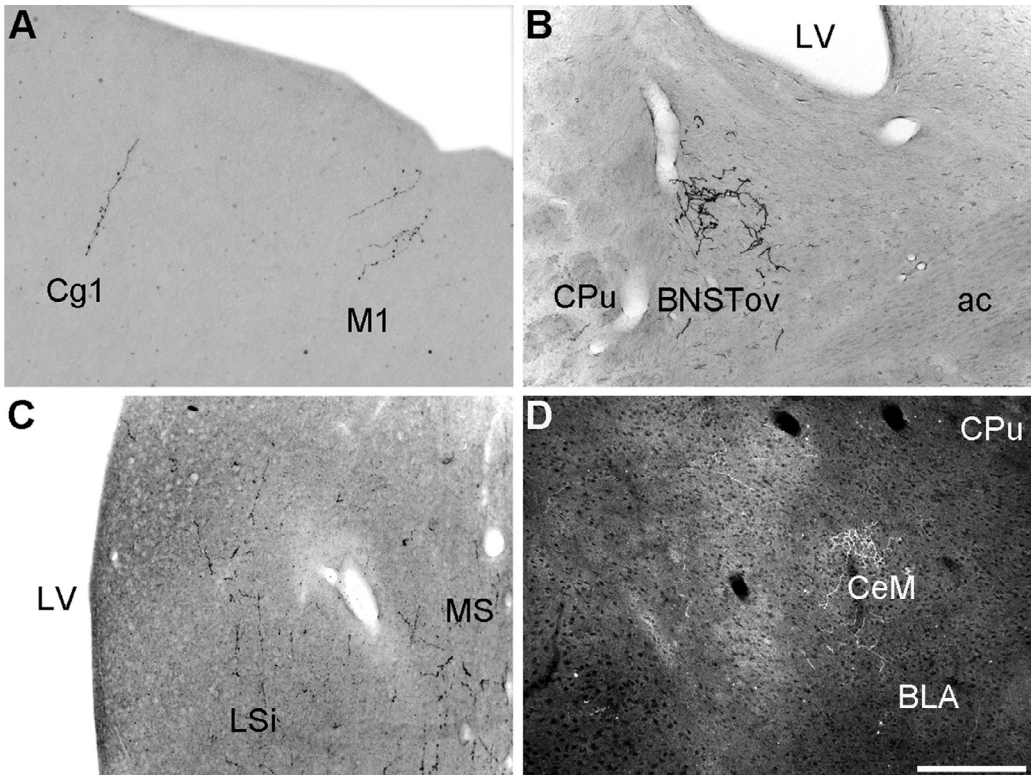


**Fig. 5.** Prosencephalic target regions of the EW. Brightfield photomicrographs of the prosencephalic regions that exhibited anterogradely BDA-labeled fibers. (A) The Cg1 displayed few anterogradely labeled fibers, and we identified fibers of passage extending branches with terminal boutons and large varicosities at this magnification. (B) A moderate number of anterogradely labeled fibers circumscribed the BNSTov. (C) A moderate number of anterogradely labeled fibers was observed in the MS and in the LSi. (D) Darkfield photomicrograph of the CeM showing a moderate number of anterogradely labeled fibers circumscribing this region. For abbreviations, see the list. Scale bar: A–D = 60 μm.

### 3.6. Spinal cord

In the spinal cord, we observed that the anterogradely labeled fibers were primarily distributed in the medial aspects of laminae VII, VIII and IX [Fig. 8C and D], extending parallel to the ventral and medial borders of the ventral horn and reaching the ventral part of the central canal in lamina X [Fig. 8F]. Anterogradely labeled fibers were also observed in laminae I, II, III and IV of the dorsal horn [Fig. 8A and B]. Moreover, we observed this labeling throughout the entire rostrocaudal axis of the spinal cord [Fig. 8].

### 3.7. Retrograde tracer control injections

After injecting CTb into the LHA of 3 animals, we observed that the boundaries of this structure were successfully targeted and that the tracer was effectively retrogradely transported to the EW in all three cases [cases LE#92, LE#93 – Fig. 9A and C – and LE#94]. In all three cases, the CTb labeling site was larger than [LE#92] or lateral to [LE#93 and LE#94] the PeF group of cells of the LHA, and in all of these cases, we observed retrogradely labeled UCN1-ir cells in the EW [Fig. 9E]. Alternatively, we injected six animals with CTb solution into the CeM and successfully targeted this structure in two cases [LE#113 and LE#114—Fig. 9B and D]. In both of these cases, we observed retrogradely CTb-labeled UCN1-ir cells in the EW [Fig. 9F]. Compared with the cases in which we injected CTb or FG into the LHA, the results from the CTb injections were superior in terms of the quality of the retrograde labeling of the EW neurons. Although the FG injections were precisely positioned in the center of the LHA [from 25 animals with FG into the LHA, we obtained six well-placed injections—LE# 49, LE# 50, LE# 51, LE# 52, LE#53 and LE# 54; but only two of these injections – LE#50 and LE#53 – exhibited very good retrograde transport to the EW—data not shown], we observed just a few retrogradely FG-labeled cells in the EW, and among those we detected double-labeled cells [FG + UCN1] [Fig. 9G and H].

### 3.8. Double-labeling in targeted EW regions

Following the injection of BDA into the EW, we examined the anterogradely labeled fibers in two target regions with respect to the role played by each region, i.e., the LHA and feeding behavior and the CeM and stress response. Therefore, we used the neuropeptides MCH and CRF as markers for relevant populations of the LHA and the CeM, respectively. In the LHA, we found MCH-ir cells that were characteristically surrounded by BDA fibers and terminal boutons adjacent to varicosities [Fig. 10C, C′ and D]. Moreover, following BDA injection into the EW, we observed anterogradely labeled fibers and terminal boutons above and surrounding the CRF-ir cells in the CeM [Fig. 10A, A′, B and B′].

## 4. Discussion

### 4.1. Anatomical aspects

In the following section, we consider the EW as a single unit to simplify the issue for the reader unless otherwise stated.

In this study, we visualized BDA fibers broadly distributed throughout the CNS following injection into the EW. Although the fibers were sparsely distributed in some regions, we observed moderate numbers of fibers concentrated in specific nuclei involved in the control of feeding behavior or stress response. We obtained six cases that we considered as good injections; i.e., BDA labeling was centered between the two parallel columns of the EW. Although we used a combination of methods

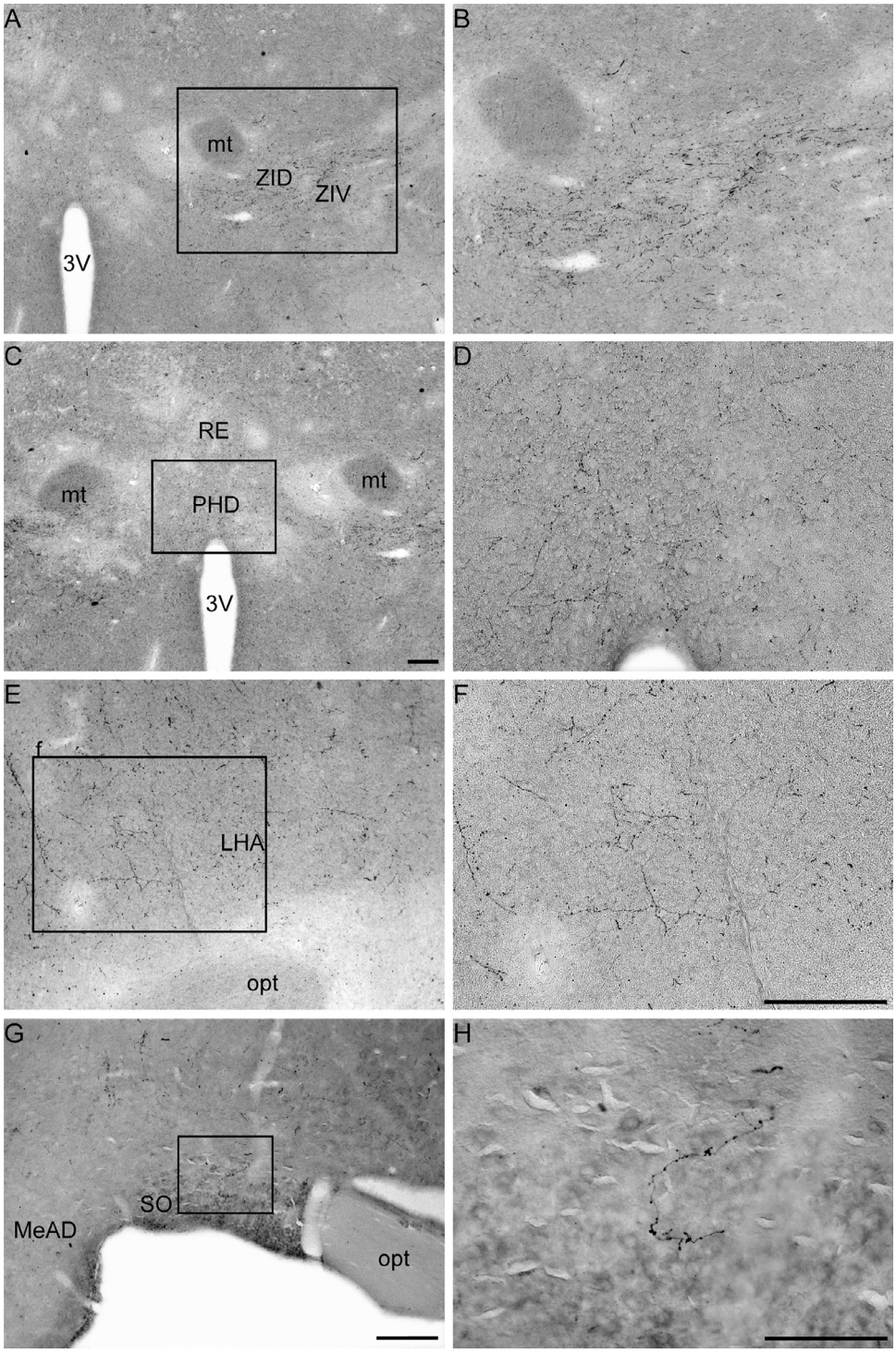


**Fig. 6.** Diencephalic target regions of the EW. Brightfield photomicrographs of the diencephalic regions that displayed anterogradely BDA-labeled fibers. The boxes drawn at the left column represent the regions on the right column in higher magnification. (A) Regions of the ZI. (B) Higher magnification of (A) presenting the details of the innervation of the dorsal [ZID] and ventral [ZIV] parts of the ZI with BDA-labeled fibers. (C) The PHD and the Re were densely innervated by BDA-labeled fibers. (D) High-power magnification of (C) showing the details of these innervations. (E) The ventrolateral part of the LHA was innervated by BDA-labeled fibers. (F) High-power magnification showing the details of the labeling shown in (E). (G) The SO was sparsely innervated by BDA-labeled fibers. (H) High-power magnification showing the details of the labeling shown in (G) and demonstrating that the fibers passing this nucleus extend many branches with terminal boutons and very large varicosities among the supraoptic magnocellular cells. For abbreviations, see the list. Scale bars: A–G = 40 μm; H = 20 μm.

[histochemistry for BDA and immunohistochemistry for UCN1] to determine whether the BDA injections targeted UCN1-ir cells, we cannot rule out the potential contamination of adjacent nuclei such as the 3N, the interstitial nucleus of Cajal, the medial accessory oculomotor nucleus and the Darkschewitsch nucleus. Nevertheless, we established that the BDA injection site was preferentially located among the UCN1-ir cells from which the efferent pathways projected to regions ranging from the prosencephalon to the spinal cord. From the classical perspective of the EW, based on the most commonly used atlases, this structure has a long rostrocaudal axis [from −5.20 to −6.84 mm to Bregma (Paxinos and Watson, 2007) or from −5.65 to −6.85 mm

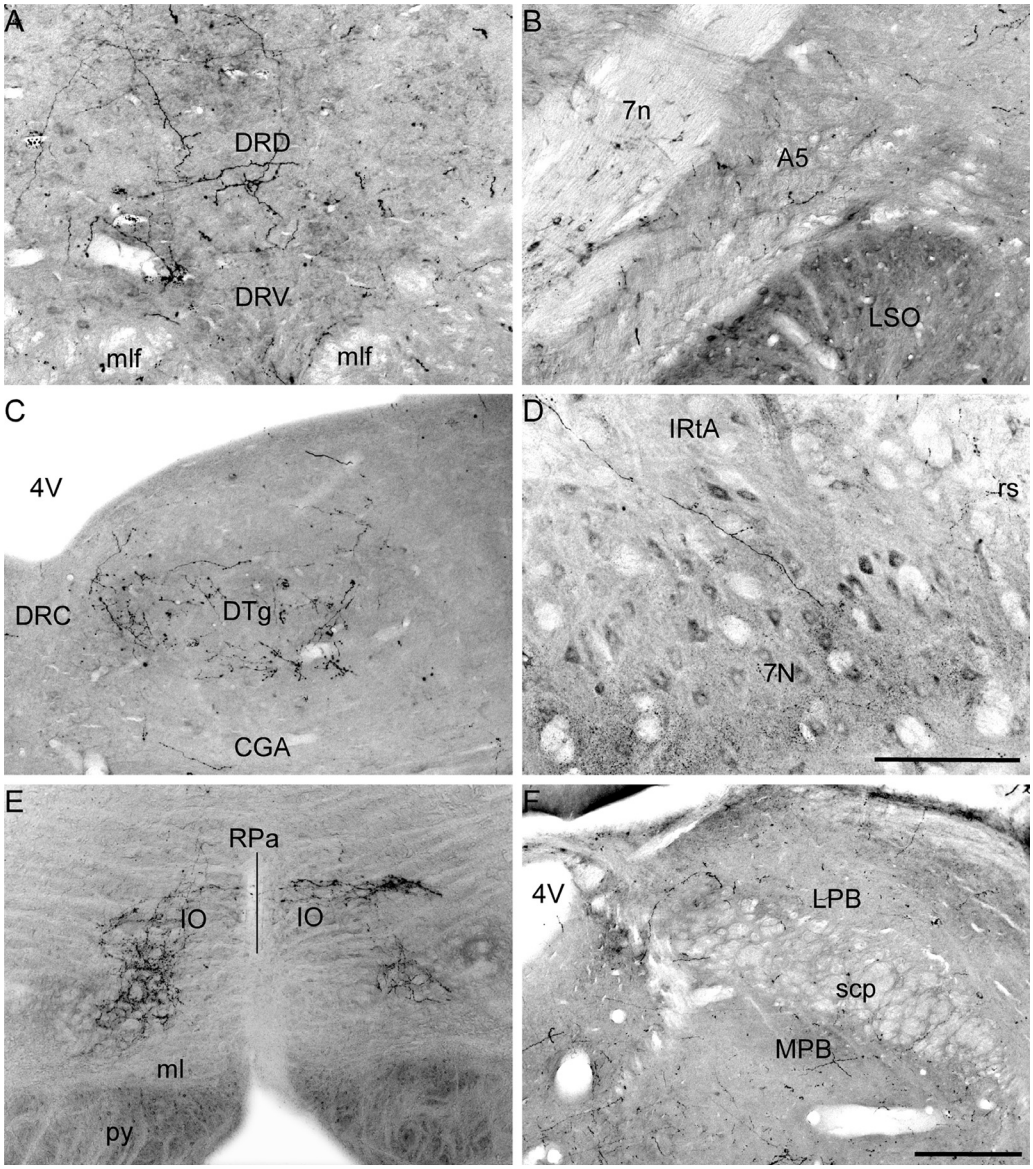


**Fig. 7.** Brainstem target regions of the EW. Brightfield photomicrographs of the brainstem nuclei displaying anterogradely BDA-labeled fibers. (A) The dorsal raphe nucleus subdivisions [dorsal and ventral parts] exhibited moderate numbers of anterogradely labeled fibers. (B) The A5 noradrenergic group of cells exhibited few anterogradely labeled fibers. (C) The DTg exhibited moderate to large numbers of anterogradely labeled fibers, primarily in the "shell" part of this nucleus. (D) The facial nucleus [7N] exhibited few BDA labeled fibers, which were observed to extend branches. (E) The IO, primarily the medial part, exhibited a very high density of BDA-labeled fibers. (F) The parabrachial nucleus, including its lateral and medial subdivisions [LPB and MPB, respectively], exhibited low to moderate numbers of BDA-labeled fibers. For abbreviations, see the list. Scale bars: A–D = 40 μm; E and F = 60 μm.

to Bregma (Swanson, 2004)]. However, the EW might expand more rostrally than these boundaries based on the detection of UCN1-ir cells in the posterior hypothalamus that were primarily ventral to the Aq (Bittencourt et al., 1999). In this regard, the extent of the long axis of the EW allowed us to demonstrate that the EW includes rostral, intermediate and caudal parts based on neurochemical signatures, cytoarchitecture and the characteristics of neighboring structures. In this study, the majority of our injections targeted a portion of the EW from approximately −5.88 to −6.12 mm relative to Bregma (Paxinos and Watson, 2007). At this location, the EW exhibits two parallel columns and an inverted trident shape (Bittencourt et al., 1999). Although this view is very difficult to observe via Nissl staining, we were able to visualize this characteristic shape using markers such as UCN1 or CART [data not shown]. Therefore, the *loci* in which we identified anterogradely labeled fibers in all six cases did not differ from each other, but the numbers of fibers differed based on the numbers of cells that absorbed the tracer, the amount of tracer that was transported, and the relative contamination from neighboring structures.

### 4.2. Functional aspects

Our findings agree with those of a previous study related to the projections of the EW to the brainstem that employed an anterograde neuronal tracer (Klooster et al., 1993). However, this is the first study to characterize the ascending projections of the EW. In addition to confirming the results of previous reports, the present study describes new targets of the EW, systematically characterizes its projections, expands the anatomical understanding of this nucleus and provides hodological bases for the understanding of EW function. Additionally, this study emphasizes the need to use anterograde tracers rather than to rely solely on the distribution maps of UCN1-ir or CART-ir fibers to examine

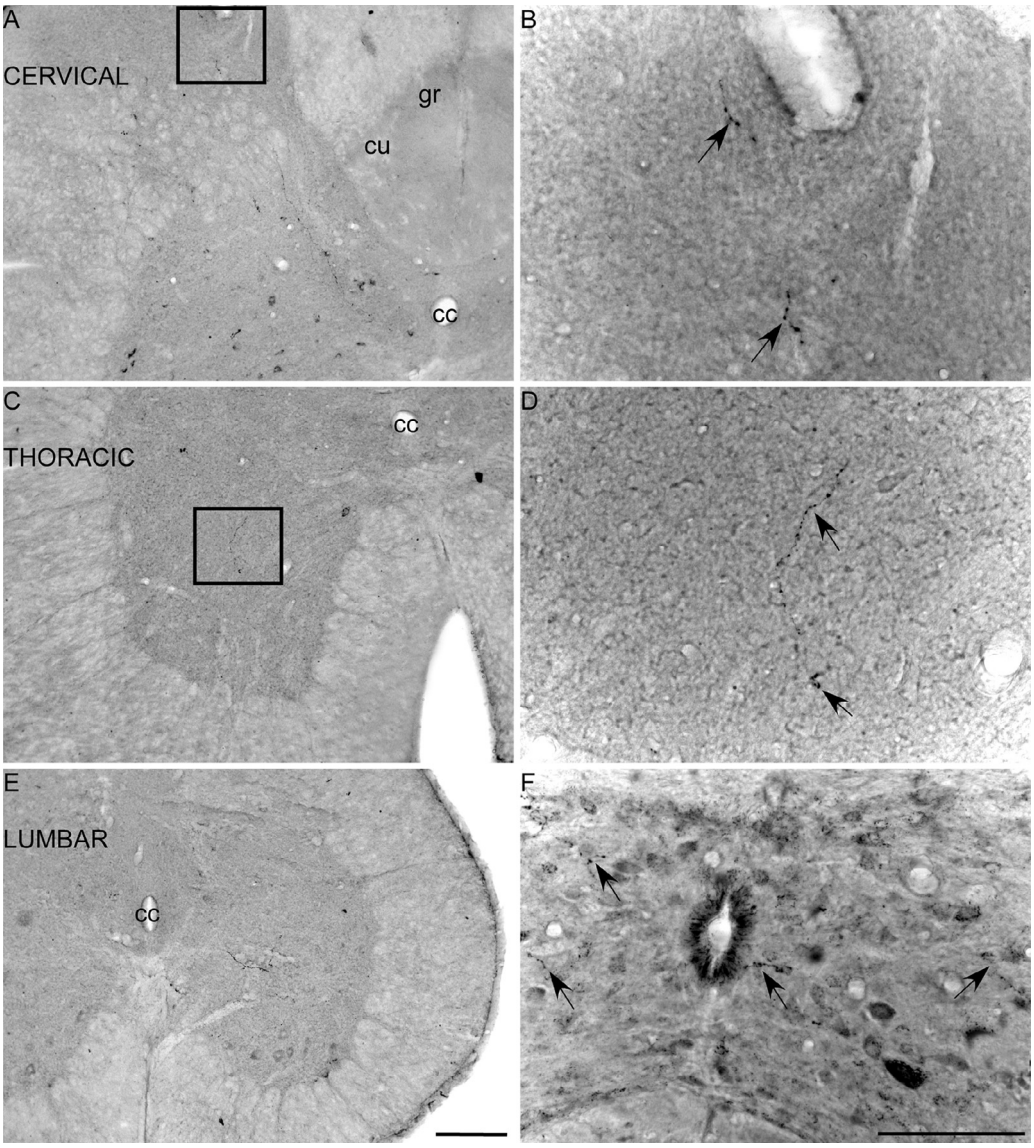


**Fig. 8.** Spinal cord target regions of the EW. Brightfield photomicrographs of various levels of the spinal cord displaying anterogradely BDA-labeled fibers in different laminae. The boxes drawn at the left column [A and C] represent the regions on the right column [B and D] in higher magnification. The part (F) of this figure is not a higher magnification of anterogradely labeled fibers presented in part (E). (A) The cervical segment of the spinal cord exhibited anterogradely labeled fibers in lamina IV. (B) Details of the highlighted area in (A) showing BDA-labeled fibers in lamina IV [black arrows]. (C) Thoracic segment of the spinal cord showing BDA-labeled fibers in lamina VIII. (D) High-power image of the highlighted area in (C) showing BDA-labeled fibers in lamina VIII [black arrows]. (E) Lumbar segment of the spinal cord showing anterogradely labeled fibers transiting from lamina VII to lamina VIII. (F) The central canal of the spinal cord was surrounded by BDA-labeled fibers, and some BDA-labeled fibers were observed at the level of the intermediomedial cell column [black arrows]. For abbreviations, see the list. Scale bars: A, C and E = 40 μm; B, D and F = 20 μm.

the projections of the EW. Notably, UCN1 is also expressed outside the EW [i.e., the LSO] (Bittencourt et al., 1999), and CART cell bodies are distributed throughout the CNS (Koylu et al., 1998; Rodrigues et al., 2011).

One of the fundamental differences between the present and previous studies is the rat strain utilized. Whereas Bittencourt et al. (1999) and Kozicz et al. (1998) used Sprague-Dawley rats [albinos], we used Long–Evans rats because they have a pigmented retina. We believe that a nucleus that is related to the eye reflex is best studied in a rat strain with accurate vision (Prusky et al., 2002). We detected fewer UCN1-ir fibers in the cerebral cortical layers in the Long–Evans rats than were detected in albino rats, and similar results were observed for the medial and lateral septal nuclei. In albino rats, moderate numbers of UCN1-ir fibers are present in the midline thalamic nuclei; in comparison, fewer fibers were observed in the Long–Evans rats. Nevertheless, the opposite pattern was observed in the BNST; we observed many UCN1-ir fibers in the Long–Evans rats, but few to moderate numbers of UCN1-ir fibers were observed in this region of Sprague-Dawley rats (Bittencourt et al., 1999; Dos Santos, 2015) [data not shown]. These findings support the hypothesis that the EW efferents of the albino and pigmented rats are different, thus demonstrating the importance of establishing the EW projections in different animal models.

As previously mentioned, UCN1 belongs to the CRF family of peptides and is therefore closely related to stress response (Cespedes et al., 2010; Gaszner et al., 2004; Kozicz et al., 2001; Weninger et al., 2000). Although UCN1 displays affinity for the $CRF_1$, it displays greater affinity for the $CRF_2$ (Vaughan et al., 1995). The primary distributions of these two receptors have been described, and they are found in different areas of the CNS (Chalmers et al., 1995; Lovenberg et al., 1995; Van Pett et al., 2000). Specifically, the major sites of $CRF_1$ mRNA expression are neocortical areas and the cerebellar cortex, whereas the major

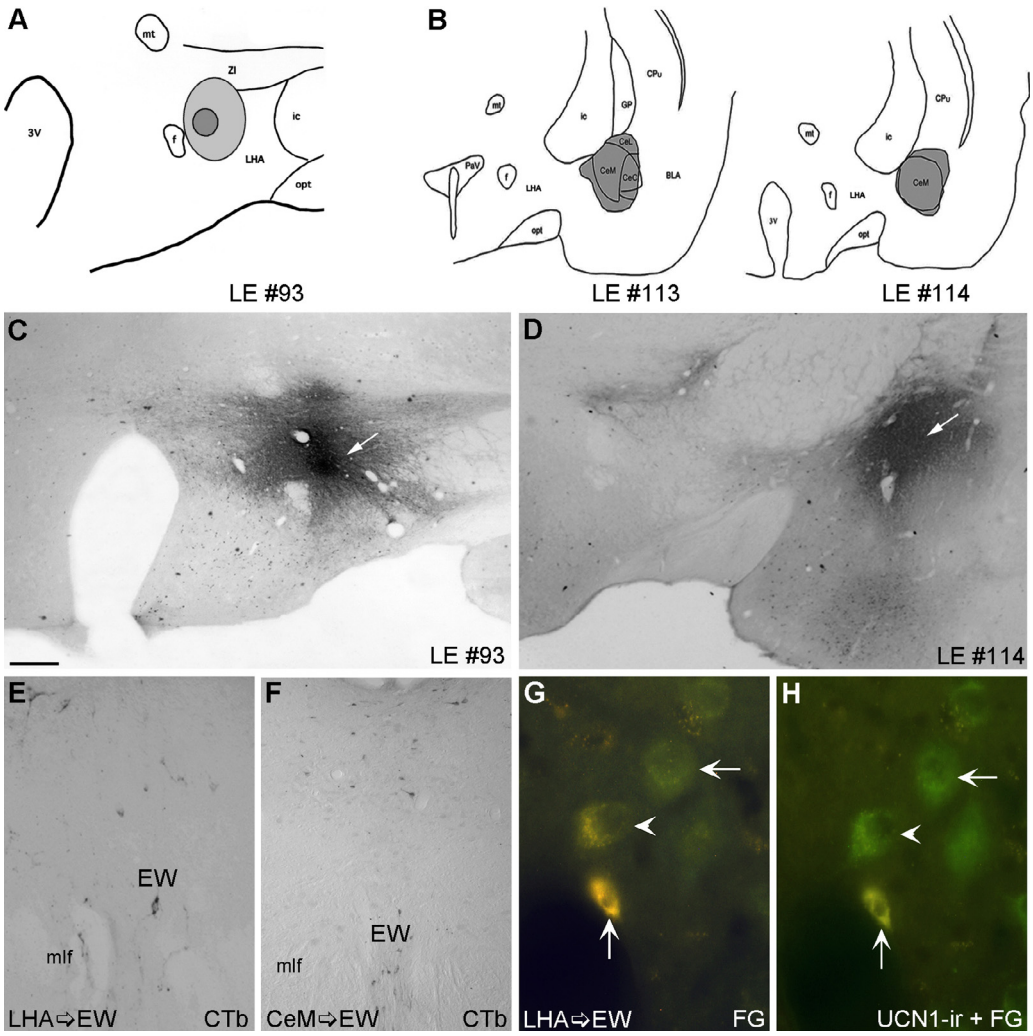


**Fig. 9.** CTb injection sites and retrogradely labeled cells in the EW. (A and B) Schematic drawings of the sites of CTb injection into the LHA [case LE#93] or the CeM [cases LE#113 and LE#114], respectively. (C) Brightfield photomicrograph of immunoperoxidase staining of the CTb injection site in the LHA [white arrow], which was localized dorsolaterally to the fornix [f] and between the fornix and the internal capsule [ic]. (D) Brightfield photomicrograph of immunoperoxidase staining of the CTb injection site in the CeM [white arrow] in case LE#114. (E) Brightfield photomicrograph of immunoperoxidase staining showing retrogradely labeled cells in the EW following CTb injection into the LHA in case LE#93. (F) Brightfield photomicrograph of immunoperoxidase staining showing retrogradely labeled cells in the EW following CTb injection into the CeM in case LE#114. (G) Fluorescence photomicrograph of retrogradely FG-labeled cells in the EW under the UV filter following the injection of FG into the LHA. (H) Immunofluorescence staining for UCN1 in retrogradely labeled cells in the EW following the injection of FG into the LHA [note that in this group of cells, there are different types of labeled cells, i.e., cells showing only FG labeling—vertical white arrow, a double-labeled cell—white arrowhead, and a cell showing only UCN1 labeling—horizontal white arrow]. For abbreviations, see the list. Scale bars: C and D = 400 μm; E and F = 200 μm; G and H = 40 μm.

sites of $CRF_2$ mRNA expression are subcortical areas such as the lateral septal nucleus, the BNST, the amygdaloid complex, the ventromedial, paraventricular and supraoptic nuclei of the hypothalamus, and, to a lesser degree, the LHA. In the present study, we found anterogradely labeled fibers ranging from few to moderate in number in all of these regions. Nonetheless, we observed anterogradely labeled fibers in regions in which neither receptor has been detected, such as the PHD. The comparison and observation of BDA labeled fibers and UCN1-ir fibers in areas of the rat CNS in which no CRF receptors have been described (Bittencourt et al., 1999; Kozicz et al., 1998) suggest that these regions contain other CRF receptors or alternative CRF receptor isoforms that have yet to be described (Donaldson et al., 1996; Vaughan et al., 1995). An alternative explanation would be that the UCN1-ir fibers contain additional neurotransmitters/neuromodulators. Thus, these fibers may activate or suppress regions that do not contain CRF receptors. Although the EW is the predominant site of UCN1 mRNA expression, some EW cells do not produce UCN1, and these cells might project to different areas than UCN1-ir cells in the EW. We cannot rule out the possibility that cells neighboring the EW captured BDA, resulting in the false detection of apparent EW targets.

We have shown in this work that EW projections are broadly distributed across the entire rostrocaudal axis of the CNS from the prosencephalon to the spinal cord. In two cases, we observed dense anterogradely labeled fibers in previously described regions including the LHA, the LSi, the RN and the BNST. Interestingly, however, the BNST innervation was only sparse in cases of injections in the intermediate EW.

We paid special attention to some of these regions exhibiting EW innervation, such as the LHA, which is classically described as a "feeding center" (Broberger et al., 1998; Elias et al., 1998; Sawchenko, 1998). In this region, we observed a moderate number of anterogradely labeled fibers surrounding MCH-ir cells; MCH is a neuropeptide that is implicated in feeding behavior (Qu et al., 1996). Although we did not examine the ultrastructural aspects of this innervation, the presence of varicose fibers and terminal boutons surrounding MCH-ir cells suggest that the

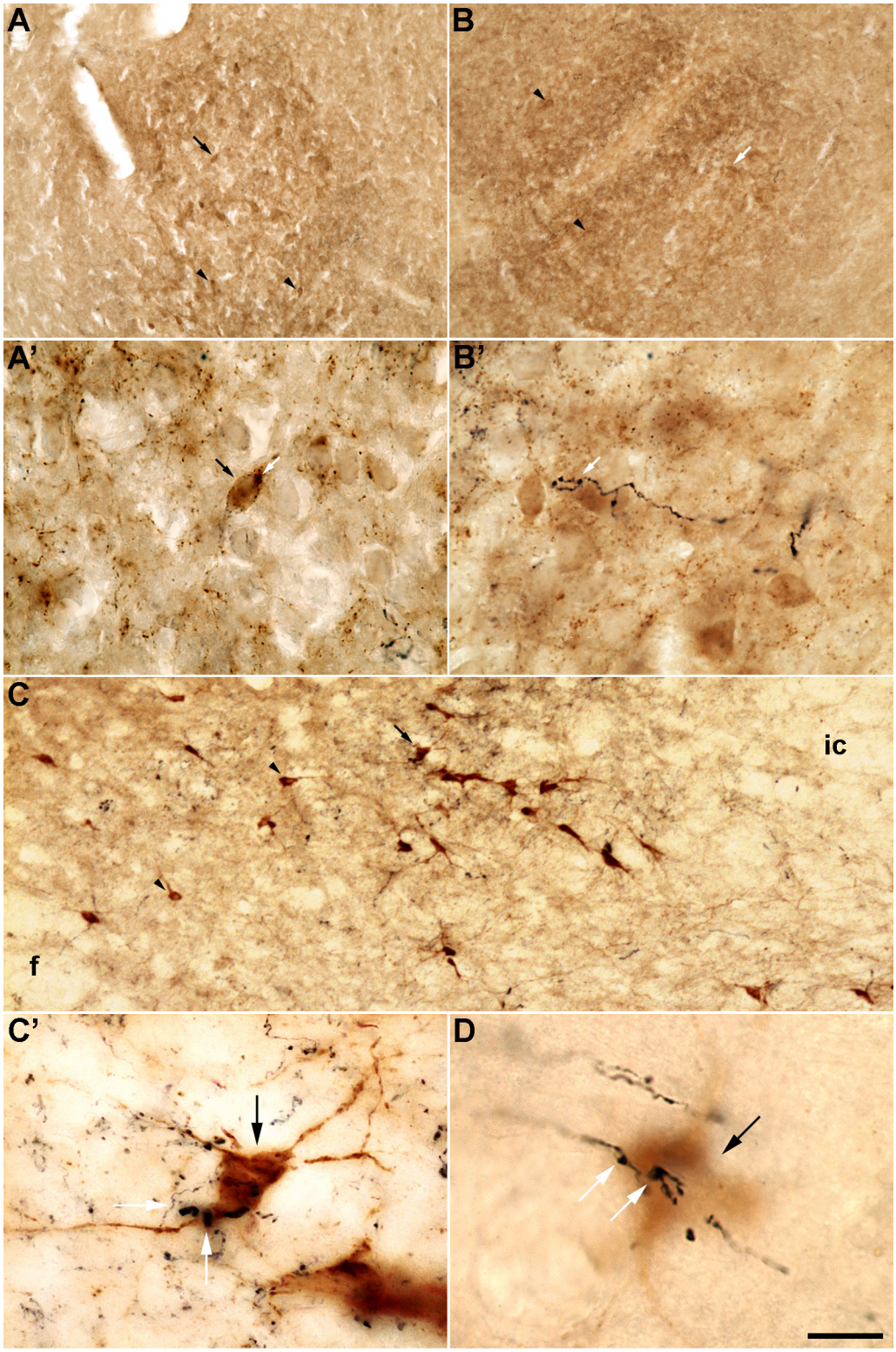


**Fig. 10.** Putative innervation of CRF-ir and MCH-ir cells by EW efferents. Brightfield photomicrographs of immunoperoxidase staining following injection of BDA into the EW. (A) CRF-ir cells in the CeM [black arrowheads] and one CRF-ir cell [as an example] surrounded by anterogradely labeled fiber [black arrow]; (A′) the same CRF-ir cell in (A) [in high power magnification—black arrow] surrounded by anterogradely labeled fiber with varicosities following the cell's contour; (B) CRF-ir cells in the CeM [black arrowheads] and one anterogradely labeled fiber [as an example—white arrow] between CRF-ir cells. (B′) the same anterogradely labeled fiber presented in (B) [in high power magnification, as an example—withe arrow] between CRF-ir cells; (C) MCH-ir cells in the LHA [black arrowheads] and one MCH-ir cell [as an example] surrounded by anterogradely labeled fiber [black arrow]; (C′) the same MCH-ir cell showed in (C) [black arrow—in high power magnification] surrounded by anterogradely labeled fibers with varicosities and terminal buttons [withe arrows] following the cell's contour; (D) a MCH-ir cell [as another example – black arrow – in high power magnification] surrounded by anterogradely labeled fiber with large varicosities and terminal buttons [white arrows] following the cell's contour. For abbreviations, see the list. Scale bars: A, B = 100 μm; A′ and B′ = 20 μm; C = 200 μm; C′ = 50 and D = 40 μm.

UCN1-expressing [i.e., anorexigenic] neurons in the EW communicate with MCH-expressing [i.e., orexigenic] neurons in the LHA. This finding may represent an anatomical basis for the involvement of the EW in feeding behavior (Qu et al., 1996; Rossi et al., 1997; Spina et al., 1996; Xu et al., 2012). The injection of the retrograde tracer CTb or FG into the LHA successfully produced retrogradely labeled cells in the EW, and we also detected cells that were clearly double-labeled with FG and UCN1-ir. Indeed, our group has described reciprocal connections between the EW and the hypothalamus, and these connections corroborate the anatomical data regarding the functional aspects of this "eye-related functional nucleus" as described in its early characterizations (da Silva et al., 2013).

The CTb injections into the CeM resulted in only a few retrogradely labeled cells in the intermediate part of the EW in two cases; however, in the other two cases, we observed many labeled neurons in the caudal part of the EW, some of which also displayed UCN1-ir [data not shown]. Our finding that EW UCN1 neurons project to the CeM is particularly interesting because the CeM has been related to the stress response, particularly conditioned fear control (Cook, 2002). Myers et al. (2005) demonstrated that implanting corticosterone pellets into the dorsal edges of the CeM evokes physical responses that are similar to those observed during stress response. When the same authors injected the $CRF_1$ antagonist antalarmin, these behavioral and physiological responses were significantly diminished. Because UCN1 also displays affinity for $CRF_1$, this connection may explain the interaction between the EW and the CeM in the stress response. Kalin et al. (2004) describes that the CeM role in mediating fear- and anxiety-related behavioral and pituitary–adrenal response to stress, including the activation of the CRF system, is similar in non-human primates [Rhesus monkey] and rodent species.

Our BDA injections revealed another new target of EW projections, the BNSTov, which receives a moderate number of well circumscribed BDA fibers. The BNST exhibits both $CRF_1$ and $CRF_2$ mRNA expression (Van Pett et al., 2000), and it is related to visceral sensory information processing and the control of feeding behavior. Therefore, it would be more appropriate to consider the circuitry between the EW and the BNSTov to be an integrative circuit of stress and feeding behavior considering the interrelated presentation of stress- and eating-related disorders (Dong et al., 2001; Micioni Di Bonaventura et al., 2014).

Our results revealed that the IO also displays very dense BDA fibers following injection of the EW. The IO has previously been described to express only small amounts of $CRF_1$ mRNA (Van Pett et al., 2000) and to be a precerebellar nucleus that receives somatosensory information that is important for cerebellar

**Table 3**
Comparison of common and "new" targets of the EW projections (based solely on the use of neuronal tracers).

| CNS regions | Loewy and Saper (1978) cat—autoradiographic and HRP | Klooster et al. (1993) rat (male Wistar)—PHA-L and retrograde tracers (fast-blue and nuclear yellow) | Bittencourt et al. (1999) rat (male Sprague-Dawley)—retrograde tracers (fast-blue and diamidino yellow) | Dos Santos (2015) – rat (male Long–Evans) – BDA and retrograde tracers (CTb and FG) |
|---|---|---|---|---|
| I. Prosencephalon/Diencephalon | | | | |
| Cerebral cortex | (−) | (−) | (−) | (+) |
| Medial and lateral septal nuclei | (−) | (−) | (+) | (+) |
| Amygdaloid complex nuclei | (−) | (−) | (−) | (+) |
| Bed nucleus of stria terminalis | (−) | (−) | (−) | (+) |
| Central nucleus of amygadala | (−) | (−) | (−) | (+) |
| Paraventricular nucleus of the hypothalamus | (−) | (−) | (−) | (+) |
| Lateral hypothalamic area | (−) | (−) | (−) | (+) |
| Thalamic nuclei | (−) | (−) | (−) | (+) |
| Zona incerta | (−) | (−) | (−) | (+) |
| Medial preoptic area | (−) | (−) | (−) | (+) |
| Reuniens thalamic nucleus | (−) | (−) | (−) | (+) |
| II. Brainstem | | | | |
| Dorsal accessory olive nucleus | (+) | (−) | (−) | (−) |
| Medial parabrachial nucleus | (+) | (−) | (−) | (+) |
| Lateral parabrachial nucleus | (−) | (+) | (−) | (+) |
| Dorsal tegmental nucleus | (−) | (−) | (−) | (+) |
| Trigeminal complex nuclei | (+) | (+) | (−) | (+) |
| Gracile and medial cuneate nuclei | (+) | (−) | (−) | (−) |
| Inferior olive nucleus | (+) | (+) | (−) | (+) |
| Principal olive nucleus | (−) | (+) | (−) | (−) |
| Medial accessory olive | (−) | (+) | (−) | (−) |
| Facial nucleus | (−) | (+) | (−) | (+) |
| Lateral reticular nucleus | (−) | (+) | (−) | (−) |
| Rostroventral reticular nucleus | (−) | (+) | (−) | (−) |
| Ciliary ganglion | (−) | (+) | (−) | (−) |
| Cerebellum (cortex and nuclei) | (−) | (−) | (−) | (−) |
| III. Spinal cord | | | | |
| Lamina I | (+) | (−) | (−) | (+) |
| Lamina II | (−) | (−) | (−) | (+) |
| Lamina III | (−) | (−) | (−) | (+) |
| Lamina IV | (−) | (−) | (−) | (−) |
| Lamina V | (+) | (−) | (−) | (−) |
| Lamina VI | (−) | (−) | (−) | (−) |
| Lamina VII | (−) | (−) | (+) | (+) |
| Lamina VIII | (−) | (−) | (−) | (+) |
| Lamina IX | (−) | (−) | (−) | (−) |
| Lamina X | (−) | (−) | (−) | (+) |

(+) Meaning structure saw with any kind of labeling. (−) Meaning without signal or not seeing.

function, e.g., the learning of discrete and sequential motor actions (Hogri et al., 2014). Because the EW is not considered to be a sensory nucleus, this projection is intriguing, and the physiological relevance of this connection is unknown. Nevertheless, we cannot discard the possibility that this terminal labeling was due to label being picked up by fibers terminating in the oculomotor nucleus that have collaterals terminating in the inferior olive.

Finally, the DTg is discussed here for two primary reasons: it received very dense and organized BDA fibers, and it was described earlier by Bittencourt et al. (1999) that this nucleus is invested with a moderate number of UCN1-ir fibers. Moreover, Lukkes et al. (2011) described scattered $CRF_2$-ir cells within the lateral and pericentral parts of the DTg at the level of the caudal dorsal raphe nucleus. The DTg is primarily related to head-direction signals, the direction system and spatial learning (Bassett and Taube, 2001). Therefore, further studies will be necessary in order to elucidate the relationship between EW/UCN1 and DTg/$CRF_2$ with the possible participation in the circuitry that controls the head-direction role in the rat.

Another interesting aspect of the EW is that a subset of its dopamine-containing neurons does not colocalize with UCN1, despite the localization of these neurons in the same nucleus. More importantly, UCN1 activity contributes to increased alcohol consumption in different species and in a gender-specific manner, independent of the direct actions of dopamine (Fonareva et al., 2009). Moreover, at present, no evidence is available regarding the particular aspects of these dopamine-containing neurons in the EW related to their projections and specific targets. However, we speculate that the target areas of these cells may be similar to those areas found in the present work, such as the CeM (Koob, 2009).

Additionally, EW innervation of laminae I, II and III of the spinal cord is predicted to be related to nociceptive control (Kato et al., 2013; Woodbury et al., 2000; Yasaka et al., 2014). Lamina VII, which was also identified as a target of the anterogradely labeled fibers, contains the intermediolateral nucleus in segments T1-L3 [preganglionic sympathetic neurons] and L6-S1 [preganglionic parasympathetic neurons] (Grant and Koerber, 2004). We also observed BDA-labeled fibers in lamina VIII, which contains the commissural inhibitory interneurons that are fundamental components of the locomotor circuitry (Wu et al., 2011). Lamina X [or area X] is a region in which we observed a high density of anterogradely labeled fibers. Lamina X, which surrounds the central canal, sends projections to the brainstem, the amygdala, the hypothalamus and the thalamus and is most likely related to visceral nociception (Wang et al., 1999). All the aforementioned laminae have been described to exhibit the coincident expression of $CRF_1$ and $CRF_2$ mRNA in mice, and this anatomical finding may corroborate the roles of the spinal cord in the stress response, the control of visceral nociceptive input, and somatomotor activity (Korosi et al., 2007).

In summary, in addition to confirming previous findings, the results of the present study identify novel targets of the projections of the EW [see Table 3 for a comparison of our results with those of previous studies that have focused on the central and peripheral projections of the EW and that utilized anterograde and retrograde tracers]. Among the observed projections, we considered the projections to the prosencephalon and the spinal cord to be particularly interesting. We speculate that the projections to the BNSTov and the CeM [CRF-expressing neurons] may be implicated in stress response and that the projections to the LHA [MCH-expressing neurons] may modulate feeding behavior. In the spinal cord, the pattern of EW innervation suggests a role of the EW in the modulation of nociception. Clearly, additional studies will be necessary to dissect the physiological relevance of EW projections to each of these specific sites.

## Conflict of interest statement

The authors report no conflicts of interest. The authors alone are responsible for the content and writing of the article.

## Acknowledgements

We would like to thank Dr. Paul E. Sawchenko, Dr. Wylie W. Vale [*in memoriam*] and Dr. Joan Vaughan from the Salk Institute for Biological Studies for the generous gifts of the antisera against UCN1, MCH and CRF. Financial support for this study was provided in the form of a grant from the *Fundação de Amparo à Pesquisa do Estado de São Paulo* [São Paulo State Foundation for the Support of Research, FAPESP; grant no. 04/13849-5] and to L.V.S. [grant no. 11/09816-8]. A.V.S. [grant no. 07/5702-2], E.D.S. [grant no. 02/11237-7], and C.A.H. [grant no. 07/56975-9] were recipients of a fellowship from FAPESP. We are also grateful to Dr. José de Anchieta de Castro e Horta Júnior for his technical support [FAPESP grant 08/02771-6]. We would also like to thank *Coordenação de Aperfeiçoamento de Pessoal de Nível Superior* [CAPES, Agency for the Advancement of Higher Education]. J.C.B. is an Investigator with the *Conselho Nacional de Desenvolvimento Científico e Tecnológico* [CNPq, National Council for Scientific and Technological Development].

## References

Akert, K., Glicksman, M.A., Lang, W., Grob, P., Huber, A., 1980. The Edinger–Westphal nucleus in the monkey. A retrograde tracer study. Brain Res. 184, 491–498.

Bachtell, R.K., Tsivkovskaia, N.O., Ryabinin, A.E., 2002. Alcohol-induced c-Fos expression in the Edinger–Westphal nucleus: pharmacological and signal transduction mechanisms. J. Pharmacol. Exp. Ther. 302, 516–524.

Bassett, J.P., Taube, J.S., 2001. Neural correlates for angular head velocity in the rat dorsal tegmental nucleus. J. Neurosci. 21, 5740–5751.

Bittencourt, J.C., Presse, F., Arias, C., Peto, C., Vaughan, J., Nahon, J.L., Vale, W., Sawchenko, P.E., 1992. The melanin-concentrating hormone system of the rat bra an immuno-hybridization histochemical characterization. J. Comp. Neurol. 319, 218–245.

Bittencourt, Vaughan, J.C., Arias, J., Rissman, C., Vale, R.A., Sawchenko, W.W.P.E., 1999. Urocortin expression in rat brain: evidence against a pervasive relationship of urocortin-containing projections with targets bearing type 2 CRF receptors. J. Comp. Neurol. 415, 285–312.

Broberger, C., De Lecea, L., Sutcliffe, J.G., Hokfelt, T., 1998. Hypocretin/orexin- and melanin-concentrating hormone-expressing cells form distinct populations in the rodent lateral hypothalamus: relationship to the neuropeptide Y and agouti gene-related protein systems. J. Comp. Neurol. 402, 460–474.

Burde, R.M., Loewy, A.D., 1980. Central origin of oculomotor parasympathetic neurons in the monkey. Brain Res. 198, 434–439.

Cespedes, I.C., de Oliveira, A.R., da Silva, J.M., da Silva, A.V., Sita, L.V., Bittencourt, J.C., 2010. mRNA expression of corticotropin-releasing factor and urocortin 1 after restraint and foot shock together with alprazolam administration. Peptides 31, 2200–2208.

Chalmers, D.T., Lovenberg, T.W., De Souza, E.B., 1995. Localization of novel corticotropin-releasing factor receptor (CRF2) mRNA expression to specific subcortical nuclei in rat brain: comparison with CRF1 receptor mRNA expression. J. Neurosci. 15, 6340–6350.

Cook, C.J., 2002. Glucocorticoid feedback increases the sensitivity of the limbic system to stress. Physiol. Behav. 75, 455–464.

Crouch, R.L., 1936. The efferent fibers of the Edinger–Westphal nucleus. J. Comp. Neurol. 64, 365–373.

da Silva, A.V., Torres, K.R., Haemmerle, C.A., Cespedes, I.C., Bittencourt, J.C., 2013. The Edinger–Westphal nucleus II: Hypothalamic afferents in the rat. J. Chem. Neuroanat. 54, 5–19.

Donaldson, C.J., Sutton, S.W., Perrin, M.H., Corrigan, A.Z., Lewis, K.A., Rivier, J.E., Vaughan, J.M., Vale, W.W., 1996. Cloning and characterization of human urocortin. Endocrinology 137, 2167–2170.

Dong, H.W., Petrovich, G.D., Watts, A.G., Swanson, L.W., 2001. Basic organization of projections from the oval and fusiform nuclei of the bed nuclei of the stria terminalis in adult rat brain. J. Comp. Neurol. 436, 430–455.

Dos Santos Jr., E., 2015. Caracterização neuroquímica e estudo das eferências do núcleo acessório do oculomotor, Anatomy. University of Sao Paulo, Sao Paulo, pp. 89 (Master Dissertation).

Douglass, J., Daoud, S., 1996. Characterization of the human cDNA and genomic DNA encoding CART: a cocaine- and amphetamine-regulated transcript. Gene 169, 241–245.

Elias, C.F., Saper, C.B., Maratos-Flier, E., Tritos, N.A., Lee, C., Kelly, J., Tatro, J.B., Hoffman, G.E., Ollmann, M.M., Barsh, G.S., Sakurai, T., Yanagisawa, M., Elmquist, J.K., 1998. Chemically defined projections linking the mediobasal hypothalamus and the lateral hypothalamic area. J. Comp. Neurol. 402, 442–459.

Fonareva, I., Spangler, E., Cannella, N., Sabino, V., Cottone, P., Ciccocioppo, R., Zorrilla, E.P., Ryabinin, A.E., 2009. Increased perioculomotor urocortin 1 immunoreactivity in genetically selected alcohol preferring rats. Alcohol. Clin. Exp. Res. 33, 1956–1965.

Gamlin, P.D., Reiner, A., 1991. The Edinger–Westphal nucleus: sources of input influencing accommodation, pupilloconstriction, and choroidal blood flow. J. Comp. Neurol. 306, 425–438.

Gaszner, B., Csernus, V., Kozicz, T., 2004. Urocortinergic neurons respond in a differentiated manner to various acute stressors in the Edinger–Westphal nucleus in the rat. J. Comp. Neurol. 480, 170–179.

Grant, G., Koerber, H.R., 2004. Spinal cord cytoarchitecture. In: Paxinos, G. (Ed.), The Rat Nervous System. third ed. Elsevier Academic Press, London, pp. 121–128.

Hauger, R.L., Grigoriadis, D.E., Dallman, M.F., Plotsky, P.M., Vale, W.W., Dautzenberg, F.M., 2003. International union of pharmacology XXXVI. Current status of the nomenclature for receptors for corticotropin-releasing factor and their ligands. Pharmacol. Rev. 55, 21–26.

Hogri, R., Segalis, E., Mintz, M., 2014. Cerebellar inhibitory output shapes the temporal dynamics of its somatosensory inferior olivary input. Cerebellum 13, 452–461.

Ishikawa, S., Sekiya, H., Kondo, Y., 1990. The center for controlling the near reflex in the midbrain of the monkey: a double labelling study. Brain Res. 519, 217–222.

Kalin, N.H., Shelton, S.E., Davidson, R.J., 2004. The role of the central nucleus of the amygdala in mediating fear and anxiety in the primate. J. Neurosci. 24, 5506–5515.

Kato, G., Kosugi, M., Mizuno, M., Strassman, A.M., 2013. Three-dimensional organization of local excitatory and inhibitory inputs to neurons in laminae III–IV of the spinal dorsal horn. J. Physiol. 591, 5645–5660.

Klooster, J., Beckers, H.J., Vrensen, G.F., van der Want, J.J., 1993. The peripheral and central projections of the Edinger–Westphal nucleus in the rat. A light and electron microscopic tracing study. Brain Res. 632, 260–273.

Koob, G.F., 2009. Brain stress systems in the amygdala and addiction. Brain Res. 1293, 61–75.

Korosi, A., Kozicz, T., Richter, J., Veening, J.G., Olivier, B., Roubos, E.W., 2007. Corticotropin-releasing factor, urocortin 1, and their receptors in the mouse spinal cord. J. Comp. Neurol. 502, 973–989.

Koylu, E.O., Couceyro, P.R., Lambert, P.D., Kuhar, M.J., 1998. Cocaine- and amphetamine-regulated transcript peptide immunohistochemical localization in the rat brain. J. Comp. Neurol. 391, 115–132.

Kozicz, T., Bittencourt, J.C., May, P.J., Reiner, A., Gamlin, P.D., Palkovits, M., Horn, A.K., Toledo, C.A., Ryabinin, A.E., 2011. The Edinger–Westphal nucleus: a historical, structural, and functional perspective on a dichotomous terminology. J. Comp. Neurol. 519, 1413–1434.

Kozicz, T., Li, M., Arimura, A., 2001. The activation of urocortin immunoreactive neurons in the Einger–Westphal nucleus following stress in rats. Stress 4, 85–90.

Kozicz, T., Yanaihara, H., Arimura, A., 1998. Distribution of urocortin-like immunoreactivity in the central nervous system of the rat. J. Comp. Neurol. 391, 1–10.

Loewy, A.D., Saper, C.B., 1978. Edinger–Westphal nucleus: projections to the brain stem and spinal cord in the cat. Brain Res. 150, 1–27.

Lovenberg, T.W., Chalmers, D.T., Liu, C., De Souza, E.B., 1995. CRF2 alpha and CRF2 beta receptor mRNAs are differentially distributed between the rat central nervous system and peripheral tissues. Endocrinology 136, 4139–4142.

Lukkes, J.L., Staub, D.R., Dietrich, A., Truitt, W., Neufeld-Cohen, A., Chen, A., Johnson, P.L., Shekhar, A., Lowry, C.A., 2011. Topographical distribution of corticotropin-releasing factor type 2 receptor-like immunoreactivity in the rat dorsal raphe nucleus: co-localization with tryptophan hydroxylase. Neuroscience 183, 47–63.

Maciewicz, R., Phipps, B.S., Foote, W.E., Aronin, N., DiFiglia, M., 1983. The distribution of substance P-containing neurons in the cat Edinger–Westphal nucleus: relationship to efferent projection systems. Brain Res. 270, 217–230.

Maciewicz, R., Phipps, B.S., Grenier, J., Poletti, C.E., 1984. Edinger–Westphal nucleus: cholecystokinin immunocytochemistry and projections to spinal cord and trigeminal nucleus in the cat. Brain Res. 299, 139–145.

May, P.J., Reiner, A.J., Ryabinin, A.E., 2008. Comparison of the distributions of urocortin-containing and cholinergic neurons in the perioculomotor midbrain of the cat and macaque. J. Comp. Neurol. 507, 1300–1316.

Micioni Di Bonaventura, M.V., Ciccocioppo, R., Romano, A., Bossert, J.M., Rice, K.C., Ubaldi, M., St Laurent, R., Gaetani, S., Massi, M., Shaham, Y., Cifani, C., 2014. Role of bed nucleus of the stria terminalis corticotrophin-releasing factor receptors in frustration stress-induced binge-like palatable food consumption in female rats with a history of food restriction. J. Neurosci. 34, 11316–11324.

Myers, D.A., Gibson, M., Schulkin, J., Greenwood Van-Meerveld, B., 2005. Corticosterone implants to the amygdala and type 1 CRH receptor regulation: effects on behavior and colonic sensitivity. Behav. Brain Res. 161, 39–44.

Nahon, J.L., Presse, F., Bittencourt, J.C., Sawchenko, P.E., Vale, W., 1989. The rat melanin-concentrating hormone messenger ribonucleic acid encodes multiple putative neuropeptides coexpressed in the dorsolateral hypothalamus. Endocrinology 125, 2056–2065.

National Research Council, 2003. Guidelines for the Care and Use of Mammals in Neuroscience and Behavioral Research. The National Academies Press, Washington, DC.

Paxinos, G., Watson, C., 2007. The Rat Brain in Stereotaxic Coordinates. Elsevier, Amsterdam.

Prusky, G.T., Harker, K.T., Douglas, R.M., Whishaw, I.Q., 2002. Variation in visual acuity within pigmented, and between pigmented and albino rat strains. Behav. Brain Res. 136, 339–348.

Qu, D., Ludwig, D.S., Gammeltoft, S., Piper, M., Pelleymounter, M.A., Cullen, M.J., Mathes, W.F., Przypek, R., Kanarek, R., Maratos-Flier, E., 1996. A role for melanin-concentrating hormone in the central regulation of feeding behaviour. Nature 380, 243–247.

Rodrigues, B.C., Cavalcante, J.C., Elias, C.F., 2011. Expression of cocaine- and amphetamine-regulated transcript in the rat forebrain during postnatal development. Neuroscience 195, 201–214.

Rossi, M., Choi, S.J., O'Shea, D., Miyoshi, T., Ghatei, M.A., Bloom, S.R., 1997. Melanin-concentrating hormone acutely stimulates feeding, but chronic administration has no effect on body weight. Endocrinology 138, 351–355.

Sawchenko, P.E., 1998. Toward a new neurobiology of energy balance, appetite, and obesity: the anatomists weigh in. J. Comp. Neurol. 402, 435–441.

Sawchenko, P.E., Swanson, L.W., Vale, W.W., 1984. Corticotropin-releasing factor: co-expression within distinct subsets of oxytocin-, vasopressin-, and neurotensin-immunoreactive neurons in the hypothalamus of the male rat. J. Neurosci. 4, 1118–1129.

Spina, M., Merlo-Pich, E., Chan, R.K., Basso, A.M., Rivier, J., Vale, W., Koob, G.F., 1996. Appetite-suppressing effects of urocortin, a CRF-related neuropeptide. Science 273, 1561–1564.

Strassman, A., Mason, P., Eckenstein, F., Baughman, R.W., Maciewicz, R., 1987. Choline acetyltransferase immunocytochemistry of Edinger–Westphal and ciliary ganglion afferent neurons in the cat. Brain Res. 423, 293–304.

Swanson, L.W., 2004. Brain Maps—Structure of the Rat Brain, third ed. Academic Press, San Diego, CA.

Van Pett, K., Viau, V., Bittencourt, J.C., Chan, R.K., Li, H.Y., Arias, C., Prins, G.S., Perrin, M., Vale, W., Sawchenko, P.E., 2000. Distribution of mRNAs encoding CRF receptors in brain and pituitary of rat and mouse. J. Comp. Neurol. 428, 191–212.

Vasconcelos, L.A., Donaldson, C., Sita, L.V., Casatti, C.A., Lotfi, C.F., Wang, L., Cadinouche, M.Z., Frigo, L., Elias, C.F., Lovejoy, D.A., Bittencourt, J.C., 2003. Urocortin in the central nervous system of a primate (Cebus apella): sequencing, immunohistochemical, and hybridization histochemical characterization. J. Comp. Neurol. 463, 157–175.

Vaughan, J., Donaldson, C., Bittencourt, J., Perrin, M.H., Lewis, K., Sutton, S., Chan, R., Turnbull, A.V., Lovejoy, D., Rivier, C., et al., 1995. Urocortin, a mammalian neuropeptide related to fish urotensin I and to corticotropin-releasing factor. Nature 378, 287–292.

Wang, C.C., Willis, W.D., Westlund, K.N., 1999. Ascending projections from the area around the spinal cord central canal: a *Phaseolus vulgaris* leucoagglutinin study in rats. J. Comp. Neurol. 415, 341–367.

Warwick, R., 1954. The ocular parasympathetic nerve supply and its mesencephalic sources. J. Anat. 88, 71–93.

Weninger, S.C., Peters, L.L., Majzoub, J.A., 2000. Urocortin expression in the Edinger–Westphal nucleus is up-regulated by stress and corticotropin-releasing hormone deficiency. Endocrinology 141, 256–263.

Woodbury, C.J., Ritter, A.M., Koerber, H.R., 2000. On the problem of lamination in the superficial dorsal horn of mammals: a reappraisal of the substantia gelatinosa in postnatal life. J. Comp. Neurol. 417, 88–102.

Wu, L., Sonner, P.M., Titus, D.J., Wiesner, E.P., Alvarez, F.J., Ziskind-Conhaim, L., 2011. Properties of a distinct subpopulation of GABAergic commissural interneurons that are part of the locomotor circuitry in the neonatal spinal cord. J. Neurosci. 31, 4821–4833.

Xu, L., Scheenen, W.J., Roubos, E.W., Kozicz, T., 2012. Peptidergic Edinger–Westphal neurons and the energy-dependent stress response. Gen. Comp. Endocrinol. 177, 296–304.

Yasaka, T., Tiong, S.Y., Polgar, E., Watanabe, M., Kumamoto, E., Riddell, J.S., Todd, A.J., 2014. A putative relay circuit providing low-threshold mechanoreceptive input to lamina I projection neurons via vertical cells in lamina II of the rat dorsal horn. Mol. Pain 10, 1–11.